A MESOPROTEROZOIC HYBRID DRY-WET AEOLIAN SYSTEM: GALHO DO MIGUEL FORMATION, SE BRAZIL

Giorgio Basilici[a,b], Áquila Ferreira Mesquita[a], Marcus Vinícius Theodoro Soares[a], Juraj Janočko[c], Nigel Philip Mountney[d], Luca Colombera[d],

[a]Department of Geology and Natural Resources, Institute of Geosciences, State University of Campinas, 13083-870, Campinas, SP, Brazil.

[b]Centro Regional de Investigaciones Científicas y Transferencia Tecnológica, La Rioja / CONICET, Argentina.

[c]Institute of Geosciences, Faculty BERG, Technical University of Kosice, Letna 9, 040 11 Kosice, Slovakia,

[d]Fluvial and Eolian Research Group, School of Earth and Environment, University of Leeds, Leeds LS2 9JT, UK

ABSTRACT

Based on Phanerozoic and present-day cases, aeolian systems are categorised into dry, wet and stabilising types. It is questioned here whether these models are applicable to Proterozoic systems when environmental conditions on the Earth's surface were markedly different. Facies and architectural-element analyses have been applied to the Mesoproterozoic aeolian succession of the Galho do Miguel Formation, SE Brazil. The aim is to identify and discuss what controlling factors govern the construction and preservation of Proterozoic aeolian systems, and to explain how these differ from Phanerozoic models. In the metaquartzarenites of Galho do Miguel Formation four aeolian subenvironments - megadunes (draas), large-scale isolated dunes with dry interdunes, small-scale isolated dunes with damp or wet interdunes and salt flats - coexisted and alternated temporally and spatially.. The construction of megadunes, large-scale dunes and dry interdunes occurred in topographically elevated areas, usually above the water table, but occasionally flooded; isolated dunes with damp and wet interdunes, and salt flats formed in low-lying areas with water table at or close to the surface.

A long-lived sediment supply combined with ongoing tectonic subsidence enabled the accumulation of a thick aeolian succession (1,000-1,500 m) that covered a large area (4,000 km^2). The water table controlled the accumulation of this unit. Where it was close to the accumulation surface, it acted to limit the availability of the wind-blown sand, hampering the construction of large and compound bedforms and allowing the deposition of damp and wet interdunes and salt flats as a wet aeolian system; Where large and compound bedforms with dry interdunes developed as a dry aeolian system, slow but progressive subsidence-driven water-table rise provided accumulation space that enabled system preservation. The Galho do Miguel Formation constitutes a hybrid aeolian system, in which both dry and wet environmental conditions were coeval.

In the Mesoproterozoic, the absence of rooted-vegetation capable of acting as a sand stabilising agent allowed the widespread generation of aeolian systems in humid as well as arid environments. In humid environmental settings, water played a significant role in the accumulation and preservation of aeolian deposits, preventing their reworking by the wind or other exogenous agents.

Key words: Dry aeolian system; wet aeolian systems; water table; erg; Espinhaço Supergroup

1. INTRODUCTION

This study examines and discusses the apparently limited architectural complexity of Precambrian aeolian depositional systems, compared to what would be expected for a

Precambrian, "bare-surface" Earth, where the action of the wind acting on plentiful source of loose and dry sediment should have been more effective at inducing complex aeolian system development (Bose et al., 2012; Rodríguez-López et al. 2014; Mesquita et al., 2021, see their Supplementary Material 1 and 2).

In principle, during the Precambrian, the absence of terrestrial vegetation that might otherwise have acted to shelter the sediment surface from wind action should have resulted in a greater abundance of aeolian depositional systems compared to the post-Silurian vegetated continent (Bose et al., 2012). However, although the absence of vegetation should have increased the availability of sand for aeolian transport and favoured the construction of large aeolian bedforms, the same absence of vegetation would have inhibited the accumulation and preservation of these bedforms. In fact, the absence of vegetation - an important sand-stabilising agent - would have left large aeolian bedforms vulnerable to erosion by winds undersaturated with respect to their potential sand-carrying capacity, else by other exogenous agents such as rivers or waves (Rodríguez-López et al., 2014; Heness et al., 2014). Eriksson and Simpson (1998) and Bose et al. (2012) argued that surface reworking by fluvial or marine processes, as well as non-recognition, are the main reasons why so few thick accumulations of aeolian succession have been identified in the Precambrian record. The role of microbial mats as stabilising agents that might potentially have acted to control aeolian construction and accumulation is generally considered insufficient to enable preservation of thick aeolian successions (Eriksson et al., 2005). However, microbial mats have been recognised in some aeolian successions that are as old as Mesoproterozoic (Simpson et al., 2013), and their influence on the stabilisation of aeolian deposits has been compared to that of present-day biological soil crusts (Basilici et al., 2020).

Current models to account for the construction, accumulation and preservation of aeolian depositional systems are mainly based on studies of modern systems and Phanerozoic sedimentary successions. Three types of aeolian system are widely identified: dry, wet and stabilising (Kocurek and Havholm, 1993; Kocurek, 1999; Mountney, 2012). Dry aeolian systems are characterised by high availability of sand for aeolian transport, such that the wind becomes saturated with respect to its potential sand-carrying capacity; downwind deceleration reduces that capacity and forces deposition of sand. In dry systems progressive sedimentation enables migratory bedforms to grow to a size whereby the interdune flat areas between dunes are eliminated; accumulation ensues as a result of the downwind climbing of the bedforms as they migrate to leave an accumulated succession (Fig. 1A). In wet aeolian systems, the water table or its capillary fringe is elevated to a level whereby it interacts with the depositional surface. The availability of sand for aeolian transport is generally lower because adhesion of sand to damp surfaces increases the sand-transport threshold of the wind. Wet aeolian systems are typically characterised by smaller dunes and broad interdune flat areas that record features of damp or wet conditions. Accumulation is controlled by a gradual but progressive water-table rise that typically occurs synchronously with downwind migration of the dunes. The gradual water-table rise can be relative in cases where the accumulation surface gradually crosses the water table due to subsidence (Fig. 1B). Examples of wet aeolian systems in Precambrian succession are described by Pulvertaft (1985), Tirsgaard and Øxnevad (1998), and Chakraborty and Sensarma (2008). In stabilising aeolian systems, biogenic, chemical and physical agents such as vegetation, microbial mats, surface crusts and cement, mud drapes and lag deposits act to protect and shield already deposited aeolian sand from potential later erosion. Stabilisation can encourage the construction of dune-scale bedforms (such as nabkhas built around plants) (Basilici and Dal' Bó, 2014). Accumulation is typically via the same stabilising factors and determines the vertical accretion of the accumulation surface. The three system types described are end-member examples; hybrid combinations of dry, wet and stabilising situations coexist in space and time (Mountney and Thompson, 2002; Mountney, 2012).

This paper examines the possible factors that led to the construction, accumulation and preservation of the Galho do Miguel Formation, produces a depositional model for this unit and seeks to explain the common occurrence of aeolian systems in humid climate setting and only the rare preservation of complex and large aeolian bedforms in Proterozoic sedimentary successions (cf. Mesquita et al., 2021; their Supplementary Material 1 and 2).

The objectives of this study are: (i) to describe the architecture of a Mesoproterozoic hybrid dry and wet aeolian system represented by the Galho do Miguel Formation; (ii) to present a model of hybrid aeolian system evolution where dry, damp and wet environments coexisted and to identify the possible controlling factors; (iii) to demonstrate the role of groundwater in controlling the construction and accumulation of a Proterozoic aeolian system; (iv) to discuss why complex and large aeolian bedforms are only very rarely preserved in Mesoproterozoic sedimentary successions.

2. GEOLOGICAL SETTING

The Galho do Miguel Formation (Pflug, 1976) is part of the Espinhaço Supergroup, which is interpreted as a sedimentary succession of a rift system formed over the São Francisco craton (Almeida et al., 2000); it is exposed in a N-S orientation for 1,200 km, crossing the states of Minas Gerais and Bahia (Fig. 2A) (Dussin and Dussin 1995; Martins Neto, 1998). In the study area, the Espinhaço Supergroup is divided into the Lower and Upper Espinhaço Basins (Chemale et al., 2012) (Fig. 2). The Lower Espinhaço Basin comprises the Bandeirinha and São João da Chapada formations and is dated to the Statherian period; the Upper Espinhaço Basin comprises the Sopa Brumadinho and Galho do Miguel formations and is dated to the Stenian period (Chemale et al., 2012; Santos et al., 2015) (Fig. 2C). During the Neoproterozoic / Pan-African orogenesis (c. 650-500 Ma.) (Chemale Jr. et al., 1993; Dussin and Dussin, 1995; Alckmim et al., 2001; Knauer, 2007; Danderfer, et al., 2009; Alkmim et al., 2017), the collision of the marginal portion of the São Francisco craton caused the deformation of the Espinhaço Supergroup, which underwent a low-grade greenschist-facies metamorphism (Chemale et al., 2012).

The Galho do Miguel Formation is exposed along the Serra do Espinhaço range for ca. 200 km in a N-S direction and ca. 20 km W-E. The structural arrangement of this unit comprises slightly asymmetrical folds with near-constant N-S strike of low-dipping beds. The reported thickness of the formation varies between 1,000 and 2,000 m (Martins-Neto, 2000; Santos et al., 2015). Our direct measurement and geological sections in the study area confirm a thickness of ca. 1,000-1,500 m. Geochronological studies on detrital zircons suggest a Stenian age (1.2-1.0 Ga) for the Galho do Miguel Formation (Chemale et al., 2012; Santos et al., 2015), implying its deposition during the post-rift stage of the Espinhaço Basin at the transition from fault-controlled to thermal subsidence stages (Martins-Neto, 1998, 2000). Low-grade metamorphism transformed the original quartzarenites of Galho do Miguel Formation into metaquartzarenite. Cross-stratified sets, 0.1 to 6 m thick, and planar parallel stratification sets, 0.1 to 6.5 m thick, are peculiar characteristics of this unit (Abrantes et al., 2020; Mesquita et al., 2021). The base of the unit is composed of marine deposits that are transgressive on the Sopa Brumadinho Formation (Dossin et al. 1987; Santos et al. 2013); the top is overlain by coastal and marine deposits (Conseilheiro Mata Group) (Santos et al., 2015). Based on detailed sedimentological study (Abrantes et al., 2020; Mesquita et al., 2021) the Galho do Miguel Formation was interpreted as the preserved record of a complex aeolian system, characterised by megadunes (draas), simples dunes and sand sheets subjected to climate-driven water-table variations, which caused temporal alternations of aeolian dune fields (ergs) and sands sheets. Based on dip-azimuth measurements of isolated transverse dune foresets, a general palaeowind direction towards E-NE has been tentatively inferred (Abrantes et al., 2020; Mesquita et al., 2021).

3. METHODS

The data considered in this paper are based on field observations, polished hand samples and thin sections. Detailed field analyses were undertaken by examining a 300 to 400 m thick part of the lower portion of the Galho do Miguel succession, along N-S trending (ca. 50 km long) and E-W trending (ca. 10-18 km wide) transects, between the town of Barão de Guaicuí and the southern portion of the National Park of the Sempre Vivas (Fig. 2B).

The sediments are exposed in natural outcrops and small quarries. Natural exposures are continuous for up to 1 km laterally and 220 m vertically. However, the expression of the natural outcrops is not entirely in the form of planar and vertical faces; additionally, *cerrado* (Brazilian savannah) vegetation partially covers some outcrop faces. It can therefore be difficult to trace sets and their bounding surfaces laterally. Quarries display vertical surfaces up to 5 m high and 30 m wide. Here, perfectly planar surfaces allow an exceptional exposure of sedimentary structures and set architectures. Metamorphism and tectonic deformation do not prevent meso- and macroscopic sedimentological field analyses: sedimentary structures from small-scale (e.g., adhesion ripples) to large-scale (e.g., cross stratified sets and cosets) are clearly visible. The low-grade metamorphism, which generated a slight overgrowth of the quartz grains, sometimes highlighted by an interlocking network, makes it difficult to document the grain size of the lithofacies in the field. However, grain-size analyses could be performed on thin sections that reveal the original outline of the grains.

The lithologically monotonous nature of the succession hampers reliable stratigraphic correlations over large distances. Thus, to correlate the studied succession between exposures, we followed outcrops that are parallel to the bed strike. Lithofacies and architectural-element analyses were undertaken on 42 outcrops. In 23 exposures, millimetre-scale measurements and facies analyses of stratigraphic sections, each from 3 to 36 m thick, were undertaken in detail. Drawings and photomosaics of 14 large two-dimensional exposures were taken to define the geometry and relationships of the lithofacies and architectural elements. Measurements of 440 sedimentary surfaces were performed using a GeoBrunton compass and Abney level with angular accuracy to within 30'. Recorded measurements are: morphological parameters of vortex ripples, dip-azimuths and angles of inclination of erosional bounding surfaces and cross-stratification surfaces. All these surfaces were restored with respect to the original palaeo-horizontal. Palaeowind orientations have been previously deduced by Abrantes et al. (2020) and Mesquita et al. (2021) to be towards N-NE; we used these data, corroborated by measurements underpinning this research, to describe the exposures of the architectural elements. The following sedimentary structures were used as reliable indicators of palaeohorizontal: (i) thin layers of irregular horizontal beds, (ii) vortex-rippled layers and (iii) erosional bounding surfaces atop compound or single sets of cross-strata when overlain by planar-parallel sandstone strata. Irregular horizontal beds were deposited on a horizontal surface of a salt flat; vortex ripples formed on horizontal subaqueous surfaces by small waves; tops of cross stratification overlain by planar lamination are erosional horizontal surfaces produced by wind. Twenty-four thin sections were used to define the lithofacies petrography, grain size and fabrics of the lithofacies. Water depth and wave period of flooded areas were estimated by measurement of grain size, crest wavelength and height, and application of the Airy wave theory, according to the methods of Immenhauser (2009). The original height of the vortex ripples was estimated by the empirical relationship proposed by Sheldon and Retallack (2001). These methods are described in detail by in Basilici et al. (2020, their Supplementary Material 1 and 2).

4. ARCHITECTURAL ELEMENTS

The Galho do Miguel Formation is characterised by well-sorted to moderately well-sorted, very fine- to coarse-grained quartzarenite (60-650 μm), with the majority of the deposits being fine- and medium-grained sandstone (150-400 μm). Monocrystalline quartz grains are dominant

(92%), followed by plagioclase (4%), microcline (3%) and sericite (1%). Five architectural element types are identified (Tab. 1) with the following primary recognition criteria: (i) compound sets of cross-strata, (ii) simple sets of cross-strata, (iii) planar-parallel sandstone strata, (iv) wavy and planar-parallel bed sandstone and (v) irregular horizontal beds. All these elements occur in the study area, but their frequency varies from south to north. The following descriptions are ordered according to genetic criteria: from dry to damp/wet conditions of deposition.

4.1. Compound sets of cross-strata (megadunes or draas)

Description

Most of the occurrences of this element are located in the southern portion of the study area, whereas few examples occur in the central and northern portions. Locally it can account for 40% of the measured section (Figs. 3 and 4), but it does not exceed 13% of the total thickness of all the measured sections. This element consists of superimposed cross-stratified sets separated by erosional surfaces, which collectively form compound cross-stratified cosets (Harms et al., 1975). The thickness of individual instances of this element varies from 4.5 to 13.5 m; the top and the bottom are erosional surfaces but the overall form of the element is tabular, albeit with frequent thickness variations along the same depositional body (Figs. 3 and 4). The maximum observable lateral extent is 500 m in an orientation interpreted previously to be palaeowind-parallel (N-NE, cf. Mesquita et al., 2021), and 230 m in a palaeowind-perpendicular orientation. Single sets of the cross-strata are 0.8-6 m thick, tabular- or trough-shaped, in sections parallel or perpendicular to the palaeowind direction, respectively. The foresets are composed of medium- to very fine-grained, moderate- to well-sorted quartz grains; they are 5-50 mm thick, 10°-22° inclined and tangential at the bottom surface. The top of this element generally is a flat erosional surface, but in places it takes the form of alternating steps and concave-up depressions onlapped by planar parallel laminations of the other architectural elements (planar-parallel laminated strata). At the base, the asymptotic toe of the foresets is in lateral continuity with planar parallel laminations of the underlying architectural element, similar to an encroaching or intertonguing contact (cf. Pulvertaft, 1985; Jones et al., 2016). In some cases, the toe of the foresets is transitional to planar wave-rippled beds (Fig. 5A).

Four different orders of erosional bounding surfaces are recognised in compound sets of cross-strata (Fig. 6). The first-order type A surface is the most extensive type of erosional surfaces separating entire elements. In palaeowind-parallel direction, it is planar or undulatory where it forms element bases and planar where it forms element tops (Figs. 7 and 8); in palaeowind-perpendicular direction, this surface is undulatory or slightly concave-up at the bottom and planar at the top (Figs. 3 and 4). The first-order type B surface separates the larger trough-shaped sets from each other. In sections perpendicular to the palaeowind direction, it is a concave-up or undulatory surface and can partially overlap the first-order type A surface (Figs. 3 and 4). In sections parallel to the palaeowind, this surface is planar and slightly inclined upwind (Fig. 8). The second-order surface is concave-up or undulatory in palaeowind-perpendicular sections (Figs. 3 and 4) and planar or slightly undulatory and concave-up in palaeowind-parallel sections (Figs. 7 and 8); it divides small trough-shaped sets from sets of similar or larger dimensions. The third-order surface occurs within the cross-stratified sets and is particularly evident in sections parallel to the dip-azimuth of the cross-strata (Fig. 7). Overall, this surface type is more steeply inclined than the directly underlying foresets and it is overlain by foresets with the same dip azimuth and angle of inclination. The mean dip-azimuths of the foresets below and above this erosional surface can vary by 20° to 90°. This type of surface is not common and it is irregularly spaced in this element.

At Serra do Pasmar (south of the study area, Fig. 2B), in a palaeowind-perpendicular section, this element consists of three large sets of trough cross-strata, 6 m high and from 60 to 100 m wide, separated by first-order type B concave-up erosional bounding surfaces (Fig. 3). The upper portion of the northern large set (left-hand site in Fig. 3) comprises a group of smaller sets of trough cross-strata (1-2 m thick and up to 30 m wide). Foreset dip-azimuths of all the trough cross-stratified sets range from 035° to 131° (mean: 091°; n: 12) (Fig. 3). At locality South of Morro Batatal (south of study area, Fig. 2B), this element type crops out in two intervals, up to 6 m thick (Fig. 4) along a palaeowind-perpendicular section that is 80 m wide. The element consists of large trough-shaped sets of cross-strata, 3-4 m thick, which are truncated relatively symmetrically on both of sides, and which are overlain by or pass laterally to smaller trough-shaped cross-strata sets, 0.8-1.8 m thick. The cross-bed dip-azimuths range from 065° to 177° (mean: 129°; n: 9) (Fig. 4). At locality North of Morro Batatal (south of study area, Fig. 2B), in a section parallel to the aeolian transport (Fig. 7), 6-9 m-thick compound sets of cross-strata exhibit tabular shape in more than 140 m of lateral extension. Larger tabular sets (5 m thick) are separated from overlying smaller sets (1 m thick) by planar erosional surfaces dipping at low-angle towards E. Foreset dip-azimuths of cross-strata range from 057° to 093° (mean: 76°; n: 17). At the locality Vargem do Padre 2 (north of the study area, Fig. 2B) (Fig. 8), a section parallel to the palaeowind direction exhibits two compound sets of cross-strata 3 to 6 m thick and more than 150 m in extent. These compound sets of cross-strata are separated by a first-order type B surface, inclined at 1.5° in up-palaeowind direction, and a thin (max 0.3 m) and discontinuous bed of wavy and planar-parallel bed sandstone. The top of the upper element is erosively overlain by a 1 m-thick bed of wavy and planar-parallel sandstone that is laterally continuous across all of the exposure. The elements are made of lenticular sets of trough cross-strata, from 0.5 to 5 m thick and from 15 to more than 40 m in lateral exten. These sets are separated by planar or slightly concave-up second-order erosional surfaces. The cross-bed dip-azimuths of the lower element range from 175° to 310°, with a mode directed toward NE (mean: 041°; n: 38); the upper element shows foresets ranging from 300° to 195° and two mains modes (NNW and ENE) (means: 107° and 324°; n: 22) (Fig. 8). At the locality Morro do Alojamento (north study area, Fig.

2B) the upper portion of an element of compound sets of cross-strata displays a convex-up erosional surface onlapped by wavy and planar-parallel bed sandstone deposits (Fig. 9).

In southern part of the study area this element type alternates frequently and repeatedly in vertical sections with planar-parallel sandstone strata and large-scale simple sets of cross-strata (Fig. 10). In contrast, in the central and northern areas, this element type is rare, and where it is identified it most commonly alternates vertically with wavy and planar-parallel beds, small-scale simple sets of cross-strata and irregular horizontal beds (Fig. 5).

Interpretation

Well-sorted, fine- to medium-grained (150-400 μm) sandstone, thick cross-stratified sets (1.5-5 m) with inclined angle of 15°-30° and tangential bottom, erosional surfaces of different orders and foreset layers with marked grain-size variations, similar to pin-stripe laminations (Fryberger and Schenk, 1988), suggest that the cross-strata of this element were deposited on the lee side of aeolian dunes of different dimensions (Hunter, 1977, 1981; Kocurek and Dott, 1981; Eriksson and Simpson, 1998; Mountney, 2006).

The first-order type A surface divides compound sets of cross-strata from architectural elements of different types (Fig. 6). It can be interpreted as a surface separating large-scale set of aeolian bedforms from widespread and thick inter-bedform deposits (see discussion below). The first-order type B surface separates the compound sets of cross-strata or simple sets of cross-strata (Fig. 6; see discussion below) climbing over each other. This can be interpreted as an interdune migration surface within an association of bedforms with reduced or absent inter-bedforms areas (Brookfield, 1977; Kocurek, 1981). The second-order surfaces are erosional forms dipping in a downwind direction (cf. Mesquita et al., 2021) originated by scouring of small bedforms (thinner cross-strata) across the flanks of the larger ones (Fig. 6). They correspond to superposition bounding surfaces (Brookfield, 1977; Kocurek, 1996). In sections parallel to the palaeowind (Figs. 7 and 8), these surfaces show a dip azimuth range of 090° corroborating the interpretation that the smaller superimposed bedforms had sinuous crestlines (Rubin and Hunter, 1983). The third-order surface corresponds to the partial erosion and geometrical variation of the lee face of the bedforms (Fig. 6). This surface is identified as a type of reactivation surface (Brookfield, 1977; Kocurek, 1996) generated by the variation of the wind flow direction (Hunter and Rubin, 1983) and/or by oblique migration of bedforms with sinuous crest lines (Kocurek et al., 2007).

The exposures of Serra do Pasmar and South of Morro Batatal show sections close to perpendicular to the palaeowind direction (Figs. 3 and 4). In both exposures, large trough cross-bedding sets are the principal characteristic of this element. These structures may be produced by transverse bedforms with out-of-phase sinuous crestline (Rubin and Carter, 2006; cf. their Fig. 34). Additionally, cross-bed dip-azimuths show a spread between 035º-177º in accordance with the computer-generated models of Rubin and Carter (2006) for this type of transverse bedform. The asymmetry of the trough-shaped set, as reported in the model of Rubin and Carter (2006), probably reflects the fact that the sections are not perfectly perpendicular to the migration vector and/or the sinuosity of the crestlines of successive dunes in a train were not perfectly out-of-phase, i.e. they exhibited the pseudorandom plan-form geometry of Rubin and Carter (2006) in relation to the phase of their along-crest sinuosity. The large trough-shaped sets are overlain by smaller trough cross-bedded sets showing similar foresets dip azimuths. These smaller sets may be interpreted as smaller transverse dunes with out-of-phase (Fig. 3) and/or in-phase sinuous crestlines (Fig. 4) superimposed on the larger parent bedform. These smaller bedforms cannot be confused with crabbing scour pits because the superimposed bedforms (i) have set dimensions that are 3 to 5 times smaller than the sets of the larger bedform, (ii) are topographically positioned in the upper part of the element that represents the overall large-scale compound bedform, and (iii) have directions of migration parallel or slightly oblique to the larger bedform migration (cf. Rubin and Hunter, 1983). This architectural element was deposited by large-scale bedforms on which smaller bedforms of similar morphological form were superimposed. Overall, the element represents the preserved deposits of compound dunes (McKee, 1979), draa (Wilson, 1973) or megadunes (Pye and Tsoar, 2009).

The sections at North of Morro Batatal and Vargem do Padre 2 (Figs. 7 and 8) are approximately parallel to the palaeowind direction. The section at North of Morro Batatal reveals the deposits of a larger bedform overlain by those of a smaller bedform; these are separated by a second-order surface, slightly inclined downwind, that can be interpreted as superposition surface (Fig. 7). At locality Vargem do Padre 2, two compound sets of cross strata are separated by an erosional surface inclined upwind (Fig. 8). Thin deposits of wavy and planar-parallel bed sandstone are preserved between these two elements. This surface, described as a first-order type B surface, can be interpreted as an interdune surface. The sets of trough cross-strata which compose the two elements constitute superimposed smaller dunes separated by second-order erosional surfaces interpretable as superposition surfaces. The greater spread of the foreset dip azimuths of the upper element compared to the lower one may indicate that the formative landform of the upper element had a more sinuous crestline. The trend of the small bedforms, superimposed on the large bedforms, can be reconstructed from the line of intersection between the mean plane of bounding surfaces scoured by small superimposed bedforms (second-order surfaces: superimposition surface) and the mean plane of foresets of the small bedforms (Rubin and Hunter, 1983). At locality North of Morro Batatal, two superposition surfaces with orientation 080°/12°NE and 169°/04°SE intersect with the mean plane of foresets to reveal reconstructed migration directions for the superimposed dunes toward 060° and 073°, respectively. These data demonstrate a uniform trend of sand transport toward ENE, parallel to perpendicular to the lee face of larger bedforms, thus confirming a pronounced crest-line sinuosity of the larger bedforms.

Collectively, these observed relationships support an interpretation for the compound sets of cross-strata as having formed by migrating transverse draas (*sensu* Havholm and Kocurek, 1988) or megadunes (*sensu* Pye and Tsoar, 2009) with sinuous crestlines, upon which superimposed smaller dunes of the same morphological type migrated obliquely over the lee-slope flanks (compound draas of McKee, 1979) (Fig. 11).

4.2. Simple sets of cross-strata (simple dunes)

Description

This architectural element consists of a single set of cross-strata with laminae that are concave-up and tangential to the bottom (Fig. 12). The foresets have dip angles of 24° to 32° and consist mainly of laminae of fine- and medium-grained sandstone, 5 to 40 mm thick, and in minor part of very fine-grained sandstone, 0.5 to 3 mm thick. Along the set, concave-up erosive bounding surfaces more or less inclined than and cutting the underlying foresets are common (Fig. 13A). The foresets resting above these erosive surfaces are concordant else exhibit low-angle downlap onto the surface; their mean foreset azimuth differs from that of the foresets by 15º-30º. Based on the thickness of this type of architectural element and its interbedding with the other types of elements, it is possible to distinguish two types of simple sets: large-scale and small-scale simple sets of cross-strata. The large-scale simple sets of cross-strata are 0.5 to 5 m thick and constitute ca. 16% in thickness of the measured sections; they commonly occur alternating with planar-parallel laminated strata and compound sets of cross-strata (Fig. 12). The small-scale simple sets of cross-strata are 0.1 to 2 m thick and constitute ca. 13% of the thickness of the measured sections; they commonly occur alternating with wavy and planar-parallel bed sandstone and irregular horizontal beds (Fig. 14). In sections parallel to the palaeowind direction, both types have tabular shape. Elements of the large-scale simple sets of cross-strata have lateral extents that exceed 500 m; elements of the small-scale sets have lateral extents up to 150 m. In transverse or oblique sections, the two types have lenticular shape (concave-up bottom and flat top): elements of the large-scale sets of cross-strata have a lateral extent of ca. 350 m and width/thickness ratio ca. 75 (Fig. 12); elements of the small-scale sets of cross-strata vary from 8 to more than 40 m in extent and their width/thickness ratio is ca. 30 (Fig. 14). In a direction parallel to the inferred palaeowind, the bottom surface is horizontal and characterised by intertonguing (encroaching, *sensu* Pulvertaft, 1985) with the underlying planar-laminated sandstones (Fig. 13B); in rare instances this contact is erosional (cf. Pulvertaft, 1985). Overall, the foreset toe passes laterally to planar parallel sandstone laminations, but in small-scale sets of cross-strata it is relatively common to observe downward transition of the foreset toe to low-angle or horizontal vortex-rippled beds (Fig. 13C). In sections perpendicular or oblique to the palaeowind direction, the erosional nature of the base is clearly evident at the lateral margins of this element (Fig. 12 and 14). The top of this element is also erosive. The top of small-scale sets of cross-strata is commonly characterised by alternating steps and depressions, 0.3 to 1.5 m wide and 0.04 to 0.4 m high, which coincide with the foreset of the cross-strata (Fig. 13D). In the large-scale sets of cross-strata, the top boundary is flat or is less commonly characterised by alternating steps and depressions. The foresets of the small-scale sets of cross-strata are, in places, characterised by soft-sediment deformation, which takes the form of symmetrical folding, as narrow anticlines and wider syncline folds (Fig. 13E). Soft-sediment deformation is also rarely observed in large-scale sets of cross-strata. Foreset dip azimuths of the large-scale simple sets of cross-strata vary from 053° to 131° with mean 083° and mode toward E, whereas small-scale sets of cross-strata display dip azimuths from 006° to 125° with mean 054° and main mode toward NE (Figs.13F and G).

The large-scale simple sets of cross-strata are common in the southern portion of the study area where they are interlayered with planar-parallel sandstone beds (Figs. 10B and 12). The small-scale sets of cross-strata are dominant in the central and northern portion of the study area; they mostly occur interlayered with the types of architectural elements wavy and planar-parallel bed sandstone and irregular horizontal beds (Figs. 5 and 14).

Interpretation

Large- and small-scale sets of cross-strata are interpreted as the preserved product of simple and isolated aeolian dunes (Figs. 15 and 16). This is supported by the following observations: (i) foreset geometry and internal organisation are similar to the compound sets of cross-strata, (ii) they are constituted by a single set and (iii) they are separated by thick interdune deposits (Kocurek, 1981; 1991). The concave-up bottom of this element, particularly evident in sections perpendicular to the palaeowind direction, is related to the erosional trough formed in front of the slipface, downwind of the line of airflow reattachment (Lancaster, 1994; Frank and Kocurek, 1996). Sinuous crestlines promoted the generation of concave-up scour pits subsequently filled by the downwind edge of the migrating dune (Mountney and Thompson, 2002; Rubin and Carter, 2007). Thus, small-scale sets of cross-strata showing marked concave-up basal bounding surface were produced by highly sinuous-crested dunes. In contrast, large-scale sets of cross-strata were the product of less markedly sinuous-crested dunes. This interpretation is supported by the foreset dip azimuth data (Figs. 13F and G). The greater spread of the foreset dip-azimuth for the small-scale cross-strata can be attributed to small transverse barchanoid dunes with pronounced along-crest sinuosity, whereas the more limited spread in large-scale cross-strata may be related to transverse barchanoid forms with less marked along-crest sinuosity. Estimations of the original dimensions of the dunes based on the methods of Kocurek and Dott (1982) and Romain and Mountney (2014) is not possible since the nature of the outcrop preclude detailed measurements of small-scale units composed of grainflow, grainfall and wind-ripple laminae. Indirectly, it can be supposed that small-scale sets of cross-strata correspond to smaller dunes due to the tighter radius of curvature of the trough cross-strata (Hunter, 1977). Most of the small-scale sets of cross-strata are found associated with the wavy and planar-parallel sandstone strata and irregular horizontal beds, which were deposited in a palaeoenvironment characterised by relatively high water table (see below). In these conditions, characterised by scarce availability of sand, small-sized dunes were generated (Havholm and Kocurek, 1994; Kocurek and Lancaster, 1999).

Sedimentary structures associated with the presence of water occur in both types of sets of cross-strata, but such features are more frequent in association with small-scale sets of cross-strata. First, irregular top surfaces of the cross-stratified sets, characterised by step and trough, are present in both large- and small-scale sets of cross-strata. This is related to erosion of damp sand where interstitial water is present (Kocurek, 1981). Second, foreset soft-sediment deformation is attributed to increases in interstitial water pressure caused by water-table rise (Doe and Dott, 1980; Horowitz, 1982; Bryant et al., 2016). Third, in many cases, the foreset toes of small-scale sets of cross-strata transitions downdip to vortex-rippled beds, demonstrating the advance of the dune slipface over a flooded area (cf. Mountney and Russell, 2009).

4.3. Planar-parallel sandstone strata (dry interdune areas)

This element constitutes ca. 11% of the thickness of the measured sections, it consists of fine- and medium-grained sandstone that forms 0.5-6.5 m thick intervals, from 50 m to more than 500 m in lateral extent parallel to the palaeowind azimuth, and from 30 to more than 300 m, in extent perpendicular to the palaeowind (Figs. 3, 7 and 12). The sandstone comprises planar horizontal, or low-angle inclined (up to 4°), parallel strata, with laminations and thin beds 1 to 20 mm thick. In natural exposures, thin laminae with grain-size variations are highlighted by differential erosion and, in thin section, it is possible to observe laminae with a crude inverse grading (Fig. 13H and 17). In some cases, small planar- or concave-up sets of cross-strata, 0.1-0.4 m thick and no more than 10 m in extent, and thin beds of symmetrical ripples occur alternating with planar-parallel strata. The erosional base of this element overlies the top of simple or compound sets of cross-strata. In some cases, the erosional top of simple dunes or draas takes the form of alternating steps and depressions and the laminations onlap the borders of the small troughs (Fig. 13D). The top portion of this element is commonly occurs intertonguing with the toe of the foresets of overlying compound or simple sets of cross-strata (Fig. 13B).

This element type is common in the southern sector of the study area, where it alternates with compound sets of cross-strata and large-scale simple sets of cross-strata (Fig. 10).

Interpretation

Planar, or low-angle, parallel strata are subcritically climbing translatent strata (Hunter, 1977) or pin-stripe laminations (Fryberger and Schenk, 1988); this interpretation is supported by the texture, crude inverse grading, thickness and geometry of the strata. These strata were deposited by climbing wind ripples on a dry depositional surface (Sharp, 1963; Hunter, 1977) (Figs. 11 and 15). Small sets of cross-strata represent infrequent small dunes with sinuous crestlines of modest lateral extent (Mountney, 2006). Symmetrical ripple beds, formed by vortex ripples, record occasional flooding across the depositional surface. The gradual transition of the toe of the foresets of the cross-strata with planar parallel strata indicates the intertonguing between grainflow and wind ripples deposits, and testifies the synchronous sedimentation of planar-parallel strata with the dune migration (Mountney and Thompson, 2002).

4.4. Wavy and planar-parallel bed sandstone (damp/wet sand sheet)

Description

Wavy and planar-parallel bed sandstone is the most common element of the Galho do Miguel Formation (ca. 45% of the thickness), It is comprised of three lithofacies: planar-parallel sandstone, wavy laminated sandstone and adhesion-ripple strata. These form a succession of tabular beds within the element, which is itself 0.1 to more than 3 m thick (Fig. 5). Rarely, it is possible to observe lenticular strata with erosional concave-up bottom and flat top, up to 0.2 m thick and more than 4 m in extent, commonly filled by wavy laminated sandstone (Fig. 18A). This element commonly occurs alternating in vertical and horizontal successions with simple sets of cross-strata and rarely with compound sets of cross-strata (Figs. 14 and 5). Wavy and planar parallel bedded sandstone and the other two architectural elements cited above typically constitute vertically stacked successions exceeding 150 m in thickness. The planar-parallel sandstone lithofacies constitutes 50-85% of the thickness of this element, and forms intervals that are 0.1-3 m thick; these deposits have been already described in the previous section. Wavy laminated sandstone constitutes 13-48% of the thickness of this element. On bedding surfaces, this lithofacies exhibits symmetrical or slightly asymmetrical ripple-scale bed forms with rectilinear and bifurcate crest-lines and peaked or rounded or flattened crests (Fig. 18B). In vertical section, this lithofacies exhibits fine-grained sandstone (130-188 μm) with foresets laminae (ca. 1 mm thick) with opposing dip directions. Laminae exhibit supercritical climbing sets with very high climb angles (Fig. 18C). Bed form spacing is 20-50 mm and decompacted height (obtained using the formula of Sheldon and Retallack, 2001; see Basilici et al., 2020, their Supplementary material) is 4-13 mm. The mean vertical form index (or ripple index) is 5.5; and the mean ripple symmetry index is 1.34. Wavy laminated sandstone forms intervals 0.1-2.9 m thick with lateral extent of more than 80 m (Fig. 18C). Adhesion ripples constitute 2% in thickness of the measured sections. However, it is likely that their scarcity is due to the difficulties in their recognition in the low-grade metamorphosed sandstone. On bedding surfaces, adhesion ripples are expressed as small asymmetrical microridges, 2 mm wide, less than 1 mm high, displaying regular spacing of 4 mm and rectilinear and/or slightly undulating crest lines (Fig. 18D). In vertical section, they are sometimes associated with tabular sets of weakly undulating and irregular cross-strata, 30-60 mm thick and with foreset inclined at angles of up to 45° and angular bottoms (Fig. 18E).

Interpretation

The planar parallel sandstone lithofacies was deposited by climbing wind ripples formed on a dry surface. The symmetrical ripples have morphological aspects (trochoidal form and vertical form index) that permit their interpretation as vortex ripples (Bagnold, 1946; Tanner, 1967; Allen, 1979; Allen, 1981) formed by waves in a subaqueous environment. By applying the Airy linear wave theory to textural and morphometric parameters of these bedforms, it was possible to reconstruct the dimension and the depth of the water bodies where these waves formed. The maximum value of wave period (T) is from 0.65 to 1.26 s and the water depth, where vortex ripples formed, was 0.04-0.5 m for T=0.65 s and 0.4-0.5 m for T=1.26 s. A wave period less than 4 s is considered typical of water masses with restricted fetch, like ponds or small lakes (Allen, 1984; Immenhauser, 2009). Flattened crests are produced by shallowing and emersion (Collinson and Mountney, 2019). Adhesion ripples on bedding surfaces correspond to the bedforms described by Glennie (1970), Kocurek and Fielder (1982) and Basilici et al. (2020), and which form when the wind transports dry sand on a damp surface. In sections perpendicular to the strike of the crestlines, the adhesion ripples appear as pseudo-cross-laminations, previously described by Hunter (1973) and Kocurek and Fielder (1982), which testify to ripple climbing in response to a rise of the capillary fringe of the water table during continuous input of sand. Lenticular strata with erosional bottom represent small scours probably provoked by localised sluggish flow of water from an interdune to another low-lying interdune (cf. Mountney and Russell, 2009). These scours remained flooded for sufficient time permitting the generation of vortex ripples (Fig. 18A). These three lithofacies alternate many times in vertical succession, indicating that, although most of the time the depositional surface was dry, frequent oscillations of the water table or occasional rainfall episodically generated a damp or flooded depositional surface. These frequent variations suggest that the water table was usually close to the depositional surface, and sometimes at the surface.

This type of architectural element alternates with deposits that record rare and probably small-scale simple dunes and draas. The intertonguing of the toe of the foresets with wavy laminated sandstone, described above, implies that the lee face of the dunes migrated toward a flooded surface, as can be observed in recent aeolian environments (Langford, 1989; Mountney and Russell, 2006, 2009).

4.5. Irregular horizontal beds (salt flat)

Description

Irregular horizontal sandstone beds represent ca. 2% of the thickness of the study sedimentary succession. However, this value is probably underestimated, due to the difficulty of recognising the sedimentary features of this element in natural outcrops. Deposits of this element type occur as flattened lenses with maximum measured thickness of 7 m and lateral extension greater than 700 m. This element is formed by a rhythmic alternation of thin white and light-grey irregular horizontal layers (Fig. 19A).

White layers compose 20-40% of the thickness of this element; they are constituted of quartz grains, 80-170 μm across (very fine- to fine-grained sandstone), and are 1-50 mm thick, on average 10 mm, and more than 30 m in lateral extent (Fig. 19A). Yet, along the same layer, the thickness is variable: the white layers show several interruptions and in some cases they occur as small flattened lenses. Six types of white layers are recognised: (i) small irregular patches, (ii) small concave-up lenses evenly spaced, (iii) thin discontinuous horizontal layers, (iv) isolated concave-up lenses, (v) humpbacked lenses and (vi) wavy lenses.

(i) Small irregular patches of white laminae "floating" in light-grey muddy sandstone sandy mudstone material constitute a common structure of this architectural element. In vertical section the patches are distributed along the same level, but they have variable thickness (<5-50 mm) and width (50-100 mm), and irregular shape and spacing. They show cuspate and jagged boundaries and their lower boundary is characterised of small protrusions of light-grey sandy mudstone material (Fig. 19B).

(ii) Small evenly spaced concave-up lenses consist of alternations of white and light-grey layers, 5-20 mm thick. They form undulated thins layers with wide synclines and narrow anticlines, less than 70 mm high and spaced 70-150 mm (Fig. 19C). Commonly, the hinge of the anticline is broken and this sedimentary structure takes the form of horizontally aligned thin concave-up lenses. In some cases, a vertical superposition of concave-up lenses is observed, similar to a pile of dishes, for a thickness of 0.2 m (Fig. 19D).

(iii) Thin discontinuous horizontal layers are 1-50 mm thick beds, characterised by frequent variations of thickness and with a lateral continuity of up to 10 m (Fig. 19A). They have the shape of flattened lenses with concave and irregular bottom and planar or rarely rippled top or weakly undulated discontinuous beds (Fig. 19A, see yellow arrow). On the same stratigraphic level, they pass to isolated concave-up lenses, described below.

(iv) Isolated concave-up lenses are 5-150 mm thick and 0.05-0.45 m wide. They consist in one or two isolated lenses showing a concave bottom and planar top; the bottom is commonly characterised by irregular and wrinkled boundaries in which the underlying light-grey layer protrudes into the bottom of the white layers forming small lobes that are 2-20 mm high (Fig. 19E). In some instances, these lenses rest erosively over older thin white layers (Fig. 19F).

(v) Humpbacked lenses are regularly spaced (14-34 mm), 8-12 mm high, arcuate and rippled lenses with the form of small humps, which develop on the same depositional surface (Fig. 19G).

(vi) Wavy lenses are observed in vertical section and on the bedding surface. In vertical section they constitute triangular and symmetrical forms with peaked crest and regular spacing. In some instances, low-angle inclined cross laminations dipping in opposing directions and climbing with sub-vertical angle are observed (Fig. 19H). On bedding surfaces symmetrical or slightly asymmetrical ripples with linear or slightly sinuous bifurcated sharp crests are present. Their decompacted height (based on the formula of Sheldon and Retallack, 2001; see Basilici et al., 2020, their Supplementary material) is 4-12 mm; the value of the spacing is 20-45 mm; the mean vertical form index (or ripple index) is 4.8; and the mean ripple symmetry index is 1.09. In some cases, it is possible to observe two generations of ripples of different scale (interference ripples). On the bedding surface, ripple continuity is in places interrupted by patches of smooth areas no larger than 0.04 m^2 (Fig. 20A). Thin, rectilinear or slightly sinuous, anastomosed cracks can be observed on the rippled bedding surface. The cracks are 3 mm wide and more than 0.7 m long. In general, they develop on the ripple crests, although in same cases they cross the ripple troughs forming a network of irregular polygons with maximum diameter of 0.15 m (Fig. 20B). The cracks also develop on the smooth areas that interrupt the continuity of wave-rippled surface (Fig. 20A).

Light-grey layers consist of grains less than 110 μm across (muddy sandstone) and constitute 60-80% of the thickness of the element (Fig. 19A, see black arrow); they are structureless, 5-150 mm thick, and more than of 30 m in lateral continuity.

Laterally and vertically, this element type passes to sets of simple set of cross strata and wavy and planar parallel bed sandstone; transitions to planar parallel sandstone strata and compound sets of cross-stratified sandstone are rarely observed. Exposures of this element type are observed in the central and northern sector of the study area (Fig. 2B).

Interpretation

Most of the deposits and sedimentary features of this type of architectural element can be related to the effects of efflorescence salt crusts on the depositional surface of a salt flat. The generic name "salt flat" is preferred to a more specific as playa or playa-lake or sabkha (Briere, 2000) due to uncertainty in defining a more specific subenvironment. Efflorescence salt crusts are saline crusts, mostly constituted of halite or gypsum, <10 to >100 mm thick, which form on the surface of a salt flat or playa-lake or sabkha (Smooth and Castens-Seidell, 1994; Goodall, 1995; Goodall et al., 2000). The evaporite deposits themselves are not usually preserved in the geological record since they are easily dissolved after original precipitation, for example by flooding, heavy rain or by rise of undersaturated capillary groundwaters. Yet, salt crusts operate directly or indirectly on the clastic sediments, trapping and deforming previous sediments (Smooth and Castens-Seidell, 1994).

The five types (i to v) of white layers formed as consequence of different types of processes associated with salt crust growth and dissolution.

(i) Small irregular patches (Fig. 19B) were deposited by wind or flooding processes on the depressions generated by bumpy growth of the salt-crust surface. Their irregular form and jagged and cuspate boundaries reflect the irregular shape of the depression amongst the salt crust (Smooth and Castens-Seidell, 1994; Goodall et al., 2000). The small dimensions of these patches (thickness and width) indicate that the efflorescence salts were characterised by a thin crust, which generated low reliefs, as observed in recent salt flats by Smooth and Castens-Seidell (1994) and Goodall et al. (2000). The small protrusions of light-grey sandy mudstone material on the lower boundaries of the patches is comparable with the "pop-corn" structure described by Smooth and Castens-Seidell (1994) and Goodall et al. (2000), which mimics the irregular surfaces of a efflorescence salt crust covered by wind- or flooding-driven sand (cf. Fig. 3C and 8A of Smooth and Castens-Seidell, 1994). These types of deposits have been described previously from both present-day environments and ancient sedimentary successions, but they were interpreted as generic sabkha deposits (Glennie, 1970; cf. his Fig. 55), salt-cemented sand (Kocurek, 1981; cf. his Fig. 21), adhesion ripples (Hubert and Hide, 1982; cf. their Fig. 3C) and trapped drifting sand between salt ridges (Fryberger et al., 1984; cf. their Figs. 8 and 9) without more specific attribution to salt crust processes.

(ii) Small, concave-up lenses that are evenly spaced (Fig. 19C) are associated with deformation of horizontal laminae for salt growth in less permeable sediment. This deformation caused the progressive bending upward of the laminae, which on the topographic surface of the playa-lake appeared as small polygon forms with forced upward margins, thus forming a tepee structures (Smooth and Castens-Seidell, 1994; Goodall et al., 2000). The irregular bottom surface is related to a "popcorn" structure, discussed above. Vertical superposition of concave-up sand lenses (Fig. 19D) resulted from the association of surface deformation and solution collapse processes (Goodall et al., 2000). The dissolution of the salt crust under the depositional surface provoked the progressive deepening of a depression below the polygonal form and successive deposition and superficial deformation of sandy laminae.

(iii) Thin discontinuous horizontal layers constitute the fill of very shallow flat depressions generated on the salt-crusted sand flat (Fig. 19A). Thin layers suggest that the depressions were shallow, which can be associated with the limited thickness of the efflorescence salt crusts (Goodall et al., 2000). Sand was carried by wind or water; in the latter case, small waves formed on temporary standing waters generated a rippled surface on the top of the horizontal layer.

(iv) Isolated concave-up lens (Figs. 17E and F) seem to have been deposited in small depressions probably produced by salt-solution collapse and/or erosion, as testified by the irregular distribution of these depressions and by the bottom cutting underlying layers. Effects of the salt growing within the sand material are testified by the buckling of the edge of the lens, which in some cases overthrusts on the edge of the adjacent lens.

(v) The origin of the humpbacked lenses (Fig. 19G) can be related to the salt-crust action. In current salt flats the efflorescent salt crusts growing on a rippled surface mimic initially the bedform morphology, but further precipitation of salt within the sand and its thermal expansion and contraction cause the overstepping of the margins and the deformation of the ripples in hump-shaped bedforms (Smooth and Castens-Seidell, 1994; Goodall et al., 2000).

(vi) The trochoidal form and vertical form index values of 2.6 justify the affinity of wavy lenses to vortex ripples produced by waves (Bagnold, 1946; Tanner, 1967; Allen, 1979; Allen, 1981). Applying the Airy linear wave theory the maximum wave period (T) is from 0.81 to 1.13 s and the water depth for the vortex ripple formation are 0.4-0.5 m for T=1.13 s and 0.075-1 m for T= 0.81 s. A wave period less than 4 s is typical of small body of standing water (Allen, 1984; Immenhauser, 2009).

In this depositional context light-grey layers may be interpreted as deposits controlled by salt-crusts growth and dissolution. Fine-grained wind-blown material (very fine sand to mud) adhered to the damp hygroscopic surfaces of the salt crusts. This material gradually accumulated on the crusts, which themselves later dissolved, for example due to rise of the undersaturated capillary groundwater or during rains and floods (cf. Goodall et al., 2000). The resultant sediment is the fine-grained and structureless light-grey layers described here.

Linear cracks in apparently cohesionless sandy deposits are not likely to develop, except in rare circumstance when the sand acquires cohesion. Microbial mats could have covered such sand surfaces with a thin film and consequently provided cohesiveness to underlying sands. Thus, these sand cracks could be the effect of desiccation and subaerial cracking of microbial mats. Schieber et al. (2007, cf. their Fig. 4(c) - 4) and Noffke (2010, cf. her Fig. III.19) attributed such features to microbial induced sedimentary structures (MISS), produced by mat-destruction features and named them 'sand cracks' or 'shrinkage cracks', respectively. The occurrence of a microbial-mat record in this type of architectural element is also suggested by the irregular distribution of vortex ripples, which occur alongside flat areas with polygonal cracks. The irregular distribution of these structures, named ripple patches (Schieber, 1998; Schieber et al., 2007), is attributed to the partial erosion of microbial mats covering a smooth surface. It can be envisaged that where the microbial mat had been ripped up, the reworking of the sand formed vortex ripples that seamlessly transitioned to smooth areas.

5. SPATIAL RELATIONSHIPS OF THE ARCHITECTURAL ELEMENTS AND DEPOSITIONAL MODEL

The five types of architectural elements show horizontal relationships that demonstrate coeval processes of deposition: (i) the toe of the foresets of compound sets of cross-strata (megadunes or draas) and large-scale simple sets of cross-strata (large-scale simple dunes) are transitional (encroaching) to the underlying planar-parallel laminated strata (dry interdune areas) (Figs. 4 and 13B); (ii) the toe of the foresets of small-scale cross-strata (small-scale simple dunes) is transitional (encroaching) to wavy and planar-parallel bed sandstone (damp/wet sand sheet) (Fig. 13C) and irregular horizontal beds (salt flat); (iii) wavy and planar-parallel bed sandstone (damp/wet sand sheet) locally onlap partially eroded compound sets of cross-strata (draas) (Fig. 9). Vertical alternations between these elements are very common: (i) alternations of compound sets of cross-strata, simple sets of cross-strata and planar-parallel bed sandstone are frequent, in some cases with thin alternation of wavy and planar-parallel bed sandstone (Figs. 5, 7, 10 and 12); (ii) wavy and planar-parallel bed sandstone is interbedded in vertical section with small-scale simple sets of cross-strata and more rarely with compound sets of cross-strata (Fig. 5); (iii) irregular horizontal beds alternate with wavy and planar-parallel bed sandstone, small-scale simple set of cross-strata and seldom with large-scale simple set of cross-strata.

Bounding surfaces of regional extent, characterised by irregular scours, palaeosols, non-aeolian deposits, polygonal sandstone cracks, evaporitic deposits or coarse-grained lag deposits, which may be attributed to temporary (or in some cases protracted) interruption of the aeolian sedimentation (i.e. the generation of super surfaces) (Kocurek, 1988, 1991; Langford and Chan, 1989, 1993; Kocurek and Havholm, 1993; Mountney, 2006), have not been observed in laterally extensive (50 km long) and thick (300-400 m) studies in this part of the Galho do Miguel Formation. The studied portion of this unit therefore appears devoid of evidence for phases of interruption of the aeolian depositional processes, marked by deep erosion (i.e. significant aeolian deflation) or sediment bypassing. Thus, this portion of the Galho do Miguel Formation seems to represent a depositional system characterised by relatively uninterrupted aeolian sedimentation. However, the restricted lateral continuity of even the largest outcrops means that supersurface representing breaks in aeolian sedimentation might be present but remain unrecognised.

The association between the five types of architectural elements likely occurred in four depositional subenvironments dominated by aeolian processes. Compound sets of cross-strata and planar-parallel sandstone strata represent compound draas (or megadunes) and coeval prevalently dry interdraas, respectively (Fig. 9). The lateral dimensions of compound sets of cross-strata, which are of the order of some hundreds of metres, demonstrate that they were isolated bedforms. Large-scale simple sets of cross-strata and planar-parallel sandstone strata correspond to a dune field of simple and isolated large-scale bedforms and coeval dry interdune areas, respectively (Fig. 15). The interpretation of planar-parallel sandstone strata as dry sand sheet deposits is unrealistic for the following reasons: (i) the bottom portion of the foresets of draas and dunes demonstrates that their deposition was coeval with the planar-parallel strata; (ii) compound sets of cross-strata (draas) and large-scale simple sets of cross-strata (large-scale dunes) alternate frequently in vertical succession with interdraa or interdune deposits and there is no evidence of interruption of sedimentation (e.g., erosional surfaces, palaeosols, coarse-grained lag deposits, polygonal cracks). Thus, there is no clear evidence for a potential transition from dry sand sheet to erg. Wavy and planar-parallel bed sandstone and small-scale simple sets of cross-strata can be identified as damp/wet sand sheet with isolated small-scale dunes (Fig. 16). Irregular horizontal beds and small-scale simple sets of cross-strata are most readily explained by the presence of salt flat with scattered small-scale dunes (Fig. 16).

The four depositional subenvironments occur across the entire study area, although a preferential distribution exists. Draas and interdraas, and large-scale simple dunes and interdunes are principally present in the southern sector of the study area, whereas damp/wet sand sheet and salt flats are more common in the central and northern parts (Fig. 2B).

6. DISCUSSION

Three end-member aeolian system types are commonly recognised: dry, wet and stabilising systems (Kocurek and Havholm, 1993). Stabilising systems are linked to agents that act to episodically or continuously protect the depositional surfaces from aeolian erosion while the system overall remains active. Common agents are vegetation, pedogenesis, cementation, coarse-grained lag deposits and mud drapes over otherwise sand-dominated surfaces (Pye and Tsoar, 1990; Kocurek and Havholm, 1993; Basilici and Dal Bó, 2010; Basilici and Dal Bó, 2014). In the Galho do Miguel efflorescence crusts, restricted to isolated and small salt flats, did not act as stabilising cement of dune surfaces, and no evidence of the influence of the other agents was observed in the lithofacies. Thus, an interpretation of a stabilised system can be excluded for this unit. Conversely, depositional conditions of dry and damp/wet environments are commonly observed in this succession. Dry and damp/wet aeolian environments are extreme examples, and intermediate situations are common (Mountney and Thompson, 2002; Mountney and Russell, 2009; Mountney, 2012). The Galho do Miguel Formation represents one of these hybrid cases where dry and damp/wet depositional conditions occur alternating in time and space. Compound draas and simple and isolate large-scale dunes divided by broad interdraas and interdune areas, respectively, constitute systems constructed in an environment that was prevalently dry. By contrast, damp/wet sand sheet and salt flat correspond to depositional areas characterised by prevalent damp and wet surface conditions. Yet, during deposition of the Galho do Miguel Formation, water was occasionally present even in mostly dry subenvironments, as previously described.

The overall absence of fluvial or marine deposits suggests a likely groundwater source, such that the dry or damp/wet conditions were determined by the position and oscillation of the water table relative to the depositional surface. The topographically elevated areas, relative to which the groundwater level was sufficiently deep so as not to allow influence on the depositional surface, were the site of construction of dry subenvironments; conversely, the low-lying areas were sites of accumulation of damp/wet sand sheet and salt flat (Fig. 21). Analogous present-day systems have been described by Mountney and Russell (2004, 2006, 2009) in Iceland, albeit with a secondary role also played by vegetation. In these areas, there are isolated small aeolian dune fields of sand constructed under essentially dry conditions and raised on a flat surface, which is characterised by a shallow groundwater and is periodically flooded. In the dry subenvironments of the Galho do Miguel Formation, the position of the groundwater had to be close to the topographic surface; large-magnitude water-table oscillations apparently affected these portions at certain times, as revealed by relatively common beds indicating depositional processes in the presence of water. Although vertical and horizontal alternations of dry and damp/wet subenvironments are common, in general an increased presence of damp/wet depositional conditions is observed towards the northern portion of the study area, possibly corresponding to a general northwards decrease of the topographic gradient (Figs. 2B and 21).

The processes that build an aeolian sedimentary succession are commonly considered in three phases: construction, accumulation and preservation (Kocurek and Havholm, 1993; Kocurek and Lancaster, 1999; Kocurek, 1999). The constructional phase depends on the strength of the wind, and the source and availability of sand. In the Galho do Miguel Formation, the wind strength is demonstrated by the presence of wind-generated bedforms. The source of sediment can be solely presumed from indirect data. In fact, non-aeolian deposits (fluvial or marine sediments) interbedded with the Galho do Miguel Formation, which could demonstrate the physical processes responsible for the supply of sand into the aeolian system, are not observed. In general, fluvial systems transport a broad spectrum of grain-size classes and petrographic components. Thus, the grain-size homogeneity and petrographic features of the sandstone suggest that a fluvial source is unlikely, and that a coastal marine source is more plausible. Longshore currents, due to their long transport path, can select the textural and mineralogical characteristics of the sediments and concentrate quartz minerals (Davies and Ethridge, 1975;

Davies, 1976; Ethridge, 1985). Marine sediments occur below the Galho do Miguel Formation and overlie this unit due to marine transgression (Santos et al., 2013, 2015); also, coeval marine environment may be suggested by the presence of salt-crust structures in irregular horizontal beds, whose origin might be related to a saline groundwater wedge that, penetrating landward and enriching the sediment pores of saline water, could produce the precipitation of salt crusts. Similarly, the Jurassic Page and Entrada Sandstone formations show occurrence of salt flat (or sabkha) deposits in areas considered to be adjacent to a marine palaeo-shoreline (Crabaugh and Kocurek, 1993; Havholm et al., 1993; Carr-Crabaugh and Kocurek, 1998).

The estimated amount of sand supplied to form the studied portion of the Galho do Miguel Formation is considerable: it exceeds a bulk of 200 km^3. The absence of stratigraphic evidence of interruption of the sedimentary processes suggests that the input of material might have been continually ongoing over a protracted time interval to enable the accumulation of this unit. Superficial features of the sand grains can be also associated with the rate of sedimentation. Sand grains of the Galho do Miguel Formation are colourless, unlike many other Proterozoic aeolian units (e.g., Dala Sandstone, Pulvertaft, 1985; Copper Formation, Taylor and Middleton, 1990; Makgabeng Formation, Simpson et al., 2013; Bandeirinha Formation, Simplício and Basilici, 2015; Venkatpur Sandstone Formation, Basilici et al., 2020), which show red or reddish brown quartz grains, due to a thin coating of iron oxides or hydroxides and clay. The formation of iron oxide and hydroxide coatings on sand grains is attributed to (i) a source of iron, (ii) a sufficiently long permanence on or near the depositional surface and (iii) alternating arid and more humid climatic conditions to permit weathering processes to precipitate iron compounds (Achyutan and Rajaguru, 1993; Walden et al., 1996; Dorn, 1998, 2013). Since a possible iron source can be identified in the mineral paragenesis (phyllosilicates, iron oxides or hydroxides associated with muddy particles, now sericite), the lack of iron coatings on sand grains in the Galho do Miguel Formation can be attributed to the absence of two other factors: a long residence time of sand grain on or near the depositional surface and climate variations between more arid and more humid conditions. The removal of previous iron oxide and hydroxide coatings on the sand grains by diagenetic or low-grade metamorphism can be excluded in the Galho do Miguel Formation, since the Bandeirinha Formation, a unit at the base of the Espinhaço Supergroup (Fig. 2C), still displays evident iron oxide and hydroxide coatings on the sand grains (Simplício and Basilici, 2015).

A high rate and volume of sediment input, the absence of clear evidence of interruptions of the sedimentary processes and low time of residence on the depositional surface of the sand grains contrast with the morphological characteristics of the aeolian system represented by the Galho do Miguel Formation. Under conditions of high sediment supply, aeolian systems are expected to construct widespread large-scale bedforms; yet, most of the Galho do Miguel Formation is composed of a damp/wet sand sheet with scattered small-scale dunes. Since the construction of large and compound bedforms depends on the availability of sand (Loope and Simpson, 1992; Kocurek and Lancaster, 1999; Kocurek, 1999), it appears that most of the sand that entered into the aeolian system of the Galho do Miguel Formation was quickly accumulated, with seemingly little opportunity for post-depositional erosion. Amongst all the factors that control sand availability, groundwater was plausibly the principal factor for the Galho do Miguel Formation system, since most of this unit (58% of thickness) is made of damp/wet sand sheet and evidence of water influence is observed in the deposits interlayered with those of bedforms formed in dry conditions.

Groundwater was not only important for controlling the sand availability and restricting the construction of draas and large-scale simple dunes, but it was also an important factor in the accumulation of the Galho do Miguel Formation. The rising groundwater table permitted not only the accumulation and preservation of damp/wet sand sheet and salt flat, but also played a significant role in defining the depositional architecture of draas and simple and isolate large-scale dunes. In dry dune fields the accumulation and preservation of interdune deposits are in general limited because the dry sand of interdune deposits is easily eroded in front of the dune in correspondence of the reattachment point of the wind flow, and can be recycled for building the next dune. As dunes climb, accumulated and preserved interdune deposits may be limited to few decimetres in thickness and a few tens of metres in lateral extent (Kocurek, 1991, 1999). By contrast, in apparently dry aeolian deposits of the Galho do Miguel interdraas and interdune deposits are up to 6.5 m thick and extend for more than 500 m. The existence of (i) vortex ripple beds interlayered within the interdune or interdraa deposits, (ii) tangential bottoms of foreset of draas that transition downward to vortex-rippled beds, (iii) alternating steps and depression at the top of the set of cross-strata and (iv) draa relicts onlapped by wavy and planar-parallel bed sandstone suggest that the water-table level was relatively close to the depositional surface in these dry subenvironments. A water-table level close to the depositional surface, but which is not elevated to a level sufficient to generate wet or damp surface conditions, and which is continuously rising can account for the accumulation of thick interdraa and interdune deposits (Havholm and Kocureck, 1994; Mountney and Jagger, 2004, see their Fig. 18A). Sand-oversaturated wind flows and extensive interdraas or interdunes may have also caused these deposits (Romain and Mountney, 2014, cf. their Fig. 10C).

Mesquita et al. (2021, cf. their Supplementary Material 1 and 2) demonstrated that Proterozoic aeolian successions, in particular those representing erg deposits, are not as common as might be expected for a land surfaces that was not influenced by the stabilising effect of the vegetation. This is probably because the absence of stabilising factors (notably vegetation) promoted the reworking of these deposits by sand-undersaturated winds, river or marine wave activity (Eriksson and Simpson, 1998; Simpson et al., 2004; Rodríguez-López et al., 2014). A groundwater level close to the depositional surface and progressively rising in parallel with the creation of accommodation by subsidence may be the key to explaining the preservation of

Proterozoic aeolian systems, most of which exhibit damp/wet (i.e. hybrid) condition of development (Rodríguez-López et al., 2014; Mesquita et al., 2021, cf. their Supplementary Material 1 and 2). Thus, the groundwater table had a dual and contrasting role in influencing the formation of the draas and large-scale dunes. First, it restricted the construction of these bedforms, reducing sand availability; second, its gradual relative rise permitted the accumulation and ultimately the preservation of deposits of draas and large-scale isolated dunes constructed in topographically elevated and dry areas.

7. CONCLUSIONS

The Galho do Miguel Formation represents a hybrid Mesoproterozoic aeolian system in which dry and damp/wet depositional conditions coexisted. Dry dune field, constituted of draas and large-scale isolated simple dune, damp/wet sand sheet and salt flat deposits are commonly interlayered throughout all the study succession, although an overall south to north trend from draas and large-scale isolated simple dune deposits to damp/wet sand sheet and salt flat deposits is observed. Dry and damp/wet conditions on the depositional surface were controlled by the level of the groundwater table: dry dune fields were constructed in topographically raised areas with deep water table level and damp/wet sand sheets and salt flats in low-lying areas with water table at or very close to the depositional surface.

The thickness and extension of the Galho do Miguel Formation associated with the absence of evidence of interruption of the aeolian depositional processes indicate that the sedimentary system received a large volume of sand via an apparently uninterrupted supply. Yet, the aeolian system was unable to construct a widespread erg consisting of large-scale bedforms, because, at least in places, the groundwater table was near the depositional surface and the sand was restricted in its availability for the sand transport.

The shallow and continuously rising ground-water table (in relative sense) inhibited the construction of a widespread erg. Yet this same characteristic also permitted the accumulation and ultimate preservation of the draas and large-scale dunes constructed in topographically raised areas. In this Mesoproterozoic environment, where the absence of stabilising factors like vegetation may have allowed rapid aeolian erosion of the dry sand of the draas and dunes, the groundwater promoted their accumulation and preservation. The shallow and probably continuously relative rise in the water table is interpreted as the main control that enables the accumulation of thick dry interdune and interdraa deposits. A shallow groundwater (but not so close to the surface to permit damp conditions) allowed for a dry depositional surface and the deposition of dry interdraa and interdune sediments; instead, the progressive and rapid rise in the groundwater level protected these deposits from erosion and enabled their accumulation.

The proposed model for this Mesoproterozoic aeolian system can account for the relative scarcity of well-developed ergs in Proterozoic depositional environments, compared with the Phanerozoic, which is significant considering the expected importance of the wind action in sculpting a barren Earth. The barren surface of the Proterozoic Earth, under the expected conditions of sand supply and wind action, should have experienced the construction and temporary accumulation of widespread ergs in dry environments. However, in absence of stabilising factors, like vegetation, sand-undersaturated wind and other physical agents (river and sea waves) were able to rework the aeolian bedforms hindering their preservation. Thus, in the Proterozoic, the accumulation and preservation of may have hinged critically on the occurrence of a groundwater table close to the depositional surface.

ACKNOWLEDGEMENTS

The authors thank the ICMBio (Instituto Chico Mendes de Conservação da Biodiversidade), the entire team of the National Park of the Sempre Vivas (Instituto Chico Mendes de

Conservação da Biodiversidade), the Casa da Gloria (Federal University of Minas Gerais), Lady Silvia Damiana de Oliveira and Mr Geraldo Damaso for cooperation and hospitality. We are also grateful to Prof. Dr. Francisco Abrantes Junior for his cooperation in the field. This work was financed by FAPESP (Fundação de Amparo à Pesquisa do Estado de São Paulo) (project number 2017/03649-9) and CNPq (Conselho Nacional de Desenvolvimento Científico e Tecnológico) (project number 2018/3062762018-6).

REFERENCES

Abrantes Jr, F.R., Basilici, G., Soares, M.V.T, 2020. Mesoproterozoic erg and sand sheet system: Architecture and controlling factors (Galho do Miguel Formation, SE Brazil). Precambrian Research 338, 105592.

Alkmim, F.F., Marshak, S., Fonseca, M.A., 2001. Assembling West Gondwana in the Neoproterozoic: clues from the São Francisco craton region, Brazil. Geology 29, 319–322.

Alkmim, F.F., Kuchenbecker, M., Reis, H.L.S., Pedrosa-Soares, A.C., 2017. The Araçuaí Belt. In: Heilbron M., Cordani U., Alkmim F. (Eds.), São Francisco Craton, Eastern Brazil. Regional Geology Reviews. Springer, Cham, pp. 255-276.

Almeida, F.F.M., Neves, B.B.B., Carneiro, C.D.R., 2000. The origin and evolution of the South American Platform. Earth-Science Reviews 50, 77–111.

Allen, J.R.L., 1979. A model for the interpretation of wave ripple-marks using their wavelength, textural composition, and shape. Journal of the Geological Society of London 136, 673-682.

Allen, P.A., 1981. Some guidelines in reconstructing ancient sea conditions from wave ripplemarks. Marine Geology 43, 59–67.

Allen, P.A., 1984. Reconstruction of ancient sea conditions with an example from the Swiss Molasse. Marine Geology 60, 455–473.

Achyutan, H., Rajaguru, S.N., 1993. Reddening of Quaternary Dune Sands from the Area of Didwana Budha Pushkar, Rajasthan - a Micromorphological Approach. Man and Environment XVI/I, 21-334.

Bagnold, R.A., 1946. Motion of waves in shallow water: interactions between waves and sand bottom. Proc. Roy. Soc. London 187, 1–15.

Basilici, G., Dal' Bo, P.F., 2010. Anatomy and controlling factors of a Late Cretaceous Aeolian sand sheet: The Marília and the Adamantina formations, NW Bauru Basin, Brazil. Sedimentary Geology 226, 71-93.

Basilici, G., Dal' Bó, P.F.F., 2014. Influence of subaqueous processes on the construction and accumulation of an aeolian sand sheet. Earth Surface Processes and Landforms 39, 1014-1029.

Basilici, G., Soares, M.V.T., Mountney, N.P., Colombera, L., 2020. Microbial influence on the accumulation of Precambrian aeolian deposits (Neoproterozoic, Venkatpur Sandstone Formation, Southern India). Precambrian Research 347, 105854.

Bose, P.K., P.G. Eriksson, S. Sarkar, D.T. Wright, P. Samanta, S. Mukhopadhyay, S. Mandal, S. Banerjee, W. Altermann, 2012. Sedimentation patterns during the Precambrian: A unique record? Marine and Petroleum Geology 33, 34-68.

Brookfield, M. E., 1977. The origin of bounding surfaces in ancient aeolian sandstones. Sedimentology 24, 303-332.

Bryant, G., Cushman, R., Nick, K., Miall, A., 2016. Paleohydrologic controls on soft-sediment deformation in the Navajo Sandstone. Sedimentary Geology 344, 205-221.

Carr-Crabaugh, M., Kocurek, G., 1998. Continental sequence stratigraphy of a wet eolian system: a key to relative sea-level change. In: Shanley, K.W., McCabe, P.J. (Eds.), Relative Role of Eustasy, Climate, and Tectonism in Continental Rocks, SEPM Special Publication 59, pp. 213-228

Chakraborty, T., Sensarma, S., 2008. Shallow marine and coastal eolian quartz arenites in the Neoarchean-Palaeoproterozoic Karutola Formation, Dongargarh Volcano-sedimentary succession, central India. Precambrian Research, 162, 284–301.

Chemale Jr., F., Alkmim, F.F., Endo, I., 1993. Late Proterozoic Tectonism in the interior of the São Francisco Craton. In: Findlay, R.H., Banks, H.R., Veevers, J.J., Unrug, R. (Eds.), Gondwana 8: assembly, evolution and dispersal. Balkema, Rotterdam, pp. 29–41.

Chemale Jr., F., Dussin, I.A., Alkmim, F.F., Martins, M.S.; Queiroga, G., Armstrong, R., Santos, M.N., 2012. Unravelling a Proterozoic basin history through detrital zircon geochronology: The case of the Espinhaço Supergroup, Minas Gerais, Brazil. Gondwana Research 22, 200-206.

CODEMIG, 2012a. Folha Diamantina. Escala 1:100000.

CODEMIG, 2012b. Folha Curimataí. Escala 1:100000.

Collinson, J.C., Mountney, N.P., 2019. Sedimentary Structures. Dunedin Academic Press, Edinburgh, fourth edition, 340 pp.

Crabaugh, M., Kocurek, G., 1993. Entrada Sandstone: an example of a wet aeolian system. In: Pye, K., (Ed.), The Dynamics and Environmental Context of Aeolian Sedimentary Systems: London, Geological Society Special Publication 72, pp. 103-126.

Danderfer, A., Waele, B., Pedreira, A.J., Nalini, H.A., 2009. New geochronological constraints on the geological evolution of Espinhaço basin within the São Francisco Craton-Brazil. Precambrian Research 170, 116-128.

Davies, D. K., 1976. Model and concepts for exploration in barrier islands. In: Sacena, R.S. (Ed.), Sedimentary environments and hydrocarbons. American Association of Petroleum Geologists, Short Course, pp. 79-115

Davies, D. K., Ethridge, F.G., 1975. Sandstone composition and depositional environment. American Association of Petroleum Geologists Bulletin, 59, 239-264.

Doe, T. W., Dott Jr, R.H., 1980. Genetic significance of deformed cross bedding--with examples from the Navajo and Weber Sandstones of Utah. Journal of Sedimentary Petrology 50, 793-812.

Dorn, R.I., 1998. Rock Coatings. Elsevier, Amsterdam, 429 pp.

Dorn, R.I., 2013. Rock coatings. In: Shroder, J. (Editor in Chief), Pope, G.A., (Ed.), Weathering and Soils Geomorphology. Treatise on Geomorphology. Academic Press, San Diego, CA, pp. 70–97.

Dossin, I.A., Garcia, A.J.V., Uhlein, A., Dossin, T.M., 1987. Facies eólico na Formação Galho do Miguel, Supergrupo Espinhaço-MG. Simp. Sist. Dep. Pré-Cambriano, Anais, Ouro Preto, pp. 85-96, (in Portuguese with English abstract).

Dussin, I.A., Dussin, T.M., 1995. Supergrupo Espinhaço: modelo de evolução geodinâmica. Geonomos 3, 19-26 (in Portuguese with English abstract).

Eriksson K.A., Simpson, E.L., 1998. Controls on spatial and temporal distribution of Precambrian eolianites. Sedimentary Geology, 120, 275–294.

Eriksson, P.G., Catuneanu, O., Sarkar, S., Tirsgaard, H., 2005. Patterns of sedimentation in the Precambrian. Sedimentary Geology, 176, 17–42.

Ethridge, F.G., 1985. Surface and subsurface methods of investigation and classification of fluvial systems. In: Flores, R.M., Ethridge, F.G., Miall, A.D., Galloway, W. E., Fouch, T.D. (Eds.) Recognition of fluvial depositional systems and their potential. SEPM, Short Course 19, pp. 9-32

Frank, A., Kocurek, G., 1996. Toward a model for airflow on the lee side of aeolian dunes. Sedimentology 43, 451-458.

Fryberger, S.G., Schenk, C.J., 1988. Pin stripe lamination: a distinctive feature of modern and ancient eolian sediments. Sedimentary Geology 55, 1-15.

Fryberger, S.G., Al-Sari, A. M., Clisham, T. J., Rizvi, S. A. R., Al-Hinai, K.G ., 1984. Wind sedimentation in the Jafurah sand sea, Saudi Arabia. Sedimentology 31, 413-431.

Glennie, K. W., 1970. Desert sedimentary environments. Developments in sedimentology 14, Elsevier publishing company, Amsterdam, London, New York, 222 pp.

Goodall, T.M., 1995. The Geology and Geomorphology of the Sabkhat Matti Region (United Arab Emirates): a Modern Analogue for Ancient Desert Sediments From North-West Europe. Unpubl. PhD Thesis, University of Aberdeen, Scotland, 433 pp.

Goodall, T.M., North, C.P., Glennie, K.W., 2000. Surface and subsurface sedimentary structures produced by salt crusts. Sedimentology 47, 99-118.

Harms J.C., Southard J.B., Spearing D.R., Walker R.G., 1975. Depositional environments as interpreted from primary sedimentary structures and stratification sequences. SEPM Short Course 2, 161 pp.

Havholm, G. K., Kocurek, G., 1988. A preliminary study of the dynamics of a modern draa, Algodones, southeastern California, USA. Sedimentology 35, 649-669.

Havholm, K.G., Kocurek, G., 1994. Factors controlling aeolian sequence stratigraphy: clues from super bounding surfaces in the Middle Jurassic Page Sandstone. Sedimentology 41, 913–934.

Havholm, K.G., Blakey, R.C., Capps, M., Jones, L., King, D.S., Kocurek, G., 1993. Correlation and significance of super bounding surfaces, eolian Jurassic Page Sandstone, Colorado Plateau, USA. In: K. Pye and N. Lancaster (Eds.) Aeolian Sediments: Ancient and Modern, Spec. Publ. Int. Ass. Sediment., 16, pp. 87–107.

Heness, E.A., Simpson, E.L., Bumby, A.J. Eriksson, P.G., Eriksson, K.A., Hilbert-Wolf, H.L., Okafor, O.J., Linnevelt, S., Malenda, H.F., Modungwa, T., 2014. Evidence for climate shifts in the ~2.0 Ga upper Makgabeng Formation erg, South Africa. Palaeogeography, Palaeoclimatology, Palaeoecology 409, 265–279.

Horowitz, D.H., 1982. Geometry and origin of large-scale deformation structures in some ancient wind-blown sand deposits. Sedimentology 29, 155–180.

Hubert J. F., Hyde M.G.,1982. Sheet-flow deposits of graded beds and mudstoaes on an alluvial sandflat-playa system: Upper Triassic Blomidon redbeds, St Mary's Bay, Nova Scotia. Sedimentology 29, 457-474.

Hunter, R.E., 1973. Pseudo-crosslamination formed by climbing adhesion ripples. Journal of Sedimentary Petrology 43, 1125-1127.

Hunter, R.E., 1977. Basic types of stratification in small eolian dunes. Sedimentology 24, 361-387.

Hunter, R.E., 1981. Stratification styles in eolian sandstones some Pennsylvanian to Jurassic examples from the western interior USA. In Ethridge Frank G. and Flores Romeo M. (Eds.), Recent and ancient nonmarine depositional environments models for exploration. SEPM Special Publication 31, pp. 315 329.

Hunter, R.E., Rubin, D.M., 1983. Interpreting cyclic crossbedding, with an example from the Navajo Sandstone. In: Brookfield, M.E., Ahlbrandt, T.S. (Eds.), Eolian sediments and processes. Elsevier, Amsterdam, pp. 428-454.

Immenhauser, A., 2009. Estimating palaeo-water depth from the physical rock record. Earth-Science Reviews 96, 107–139.

Jones F. H., Scherer, C.M.S., Kuchle, J., 2016. Facies architecture and stratigraphic evolution of aeolian dune and interdune deposits, Permian Caldeirão Member (Santa Brígida Formation), Brazil. Sedimentary Geology 337, 133-150

Knauer, L.G., 2007. O Supergrupo Espinhaço em Minas Gerais: considerações sobre sua estratigrafia e seu arranjo estrutural. Geonomos 15, 81-90 (in Portuguese with English abstract).

Kocurek, G., 1981. Significance of interdune deposits and bounding surfaces in aeolian dune sands. Sedimentology 28, 753–780.

Kocurek, G., 1988. First-order and super bounding surfaces in eolian sequences - Bounding surfaces revisited. Sedimentary Geology 56, 193-206.

Kocurek, G., 1991. Interpretation of ancient eolian sand dunes. Annual Review Earth and Planetary Sciences 19, 43-75.

Kocurek, G., 1996. Desert aeolian systems. In: Reading, H.G. (Ed.), Sedimentary Environments: Processes, Facies and Stratigraphy. Third Edition. Blackwell Science, Oxford, UK, pp. 125-153.

Kocurek, G., 1999. The Aeolian rock record (Yes, Virginia, it exists, but it really is rather special to create one). In: Goudie, A.S., Livingstone, I. (Eds.), Aeolian Environments, Sediments and Landforms, John Wiley and Sons, Chichester, pp. 239-259.

Kocurek, G., Dott, R.H., 1981. Distinctions and uses of stratification types in the interpretation of eolian sand. Journal of Sedimentary Petrology 51, 579–595.

Kocurek, G., Fielder, G., 1982. Adhesion structures. Journal od Sedimentary Petrology 52, 1229-1241.

Kocurek, G., Havholm, K.G., 1993. Aeolian sequence stratigraphy - a conceptual framework. In: P. Weimer, H. Posamentier (Eds.), Siliciclastic Sequence Stratigraphy. Recent Developments and Applications. American Association of Petroleum Geologists Memoir 58, pp. 393–409.

Kocurek, G., Lancaster, N., 1999. Aeolian system sediment state: theory and Mojave Desert Kelso dune field example. Sedimentology 46, 505–515.

Kocurek, G., Mary Carr, Ryan Ewing, Karen G. Havholm, Y.C. Nagar, A.K. Singhvi, 2007. White Sands Dune Field, New Mexico: Age, dune dynamics and recent accumulations. Sedimentary Geology 197, 313–331

Lancaster, N., 1994. Dune morphology and dynamics. In: Abrahalrls, A.D., Parsons, A. J. (Eds.) Geomorphology of desert environments. Springer-Science+Business Media, B.Y., pp. 474-505.

Langford, R.P., 1989. Fluvial-aeolian interactions: Part I, modern systems. Sedimentology 36, 1023-1035

Langford, R.P. and Chan, M.A., 1989. Fluvial-aeolian interactions: part 2, ancient systems. Sedimentology 36, 1037–1051.

Langford, R.P., Chan, M.A., 1993. Downwind changes within an ancient dune sea: Permian Cedar Mesa Sandstone, southeast Utah. In: Pye, K. and Lancaster, N. (Eds.) Aeolian Sediments Ancient and Modern, Spec. Publ. Int. Assoc. Sedimentol. 16, pp. 109–126.

Loope, D.B., Simpson, E.L., 1992. Significance of thin sets of eolian cross-strata. Journal of Sedimentary Petrology 62, 849--859.

Martins-Neto, M.A., 1998. O Supergrupo Espinhaço em Minas Gerais: registro de uma bacia rifte-sag do Paleo/Mesoproterozóico. Revista Brasileira de Geociências 28, 151-168. (in Portuguese with N. Tectonics and sedimentation in a Paleo/Mesoproterozoic rift-sag basin (Espinhaço basin, southeastern Brazil). Precambrian Research 103, 147-173.

McKee, E. D., 1966. Structures of dunes at White Sands National Monument, New Mexico. Sedimentology, 7, 3–69.

McKee, E. D., 1979. Introduction to a study of global sand seas. In McKee, E. D. (Ed.), A study of global sand seas. Prof. Pap. US Geol. Surv. 1052, pp. 1–19.

Mesquita, A.F., Basilici, G., Soares, M.V.T. Garcia, R.G.V., 2021. Morphology, accumulation and preservation of draa systems in a Precambrian erg (Galho do Miguel Formation, SE Brazil). Sedimentary Geology 412, 105807.

Mountney, N. P., 2012. A stratigraphic model to account for complexity in aeolian dune and interdune successions Sedimentology 59, 964–989.

Mountney, N.P., 2006. Eolian facies models. In: Posamentier, H.W., Walker, R.G. (Eds.), Facies models revisited: Society for Sedimentary Geology Special Publication 84, 19–83.

Mountney, N.P., Russell, A. J., 2004. Sedimentology of cold-climate aeolian sandsheet deposits in the Askja region of northeast Iceland. Sedimentary Geology 166, 223-244.

Mountney, N.P., Russell, A. J., 2006. Coastal aeolian dune development, Sólheimasandur, southern Iceland. Sedimentary Geology 192, 167–181.

Mountney, N.P., Russell, A. J., 2009. Aeolian dune-field development in a water table-controlled system: Skeiđarársandur, Southern Iceland. Sedimentology 56, 2107–2131.

Mountney, N.P., Thompson, D.B., 2002. Stratigraphic evolution and preservation of aeolian dune and damp/wet interdune strata: an example from the Triassic Helsby Sandstone Formation, Cheshire Basin, UK. Sedimentology 49, 805–833.

Mountney, N.P., Jagger, A., 2004. Stratigraphic evolution of an aeolian erg margin system: the Permian Cedar Mesa Sandstone, SE Utah, USA. Sedimentology 51, 713–743.

Noffke, N., 2010. Microbial mats in sandy deposits. Elsevier, Amsterdam, 196 pp.

Pflug, R., 1968. Observações sobre a estratigrafia da Série Minas na região de Diamantina, Minas Gerais. Boletim da Divisão de Geologia e Mineralogia do Departamento Nacional de Produção Mineral: Notas Preliminares 142, 20 pp. (in Portuguese).

Pulvertaft, T.C.R., 1985. Aeolian dune and wet interdune sedimentation in the middle Proterozoic Dala sandstone, Sweden. Sedimentary Geology 44, 93-111.

Pye, K., Tsoar, H., 2009. Aeolian Sand and Sand Dunes. Springer-Verlag Berlin Heidelberg, 458 pp.

Rodríguez-López, J. R., Clemmensen, L. B., Lancaster, N., Mountney, N. P., Veiga, G. D., 2014. Archean to Recent aeolian sand systems and their sedimentary record: Current understanding and future prospects. Sedimentology 61, 1487-534

Romain, H., Mountney, N.P., 2014. Reconstruction of three-dimensional eolian dune architecture from one-dimensional core data through adoption of analog data from outcrop. American Association of Petroleum Geologists Bulletin 98, 1-22.

Rubin, D.M., Carter, C.L., 2006. Cross-bedding, bedforms, and paleocurrents. SEPM Concepts Sedimentol. Paleontol. 1, 2nd edn, 195 pp.

Rubin, D.M., Hunter, R.E., 1983, Reconstructing bedform assemblages from compound crossbedding. In Brookfield, M.E., Ahlbrandt, T.S. (Eds.), Eolian sediments and processes. Elsevier, Amsterdam, pp. 407-427.

Santos M.N., Chemale Jr., F., Dussin, I.A., Martins, M., Assis, T.A.R., Jelinek, A.R., Guadagnin, F., Armstrong, R., 2013. Sedimentological and Paleoenvironmental Constraints of the Statherian and Stenian Espinhaço Rift System, Brazil. Sedimentary Geology 290, 47-59.

Santos, M.N, Chemale Jr, F., Dussin, I.A., Martins, M.S., Queiroga, G., Pinto, R.T.R., Santos, A.N., Armstrong, R., 2015. Provenance and paleogeographic reconstruction of a Mesoproterozoic intracratonic sag basin (Upper Espinhaço Basin, Brazil). Sedimentary Geology 318, 40-57.

Schieber, J., 1989. Possible indicators of microbial mat deposits in shales and sandstones: examples from the Mid-Proterozoic Belt Supergroup, Montana, U.S.A. Sedimentary Geology 120, 105–124.

Schieber, J., P.K. Bose, P.G. Eriksson, S. Banerjee, S. Sarkar, W. Altermann, O. Catuneanu (Eds.), 2007. Atlas of Microbial Mat Features Preserved within the Clastic Rock Record. Elsevier, Amsterdam, 311 pp.

Sharp, R.P., 1963. Wind Ripples. The Journal of Geology 71, 617-636.

Sheldon, N.D., Retallack, G.J., 2001. Equation for compaction of palaeosols due to burial. Geology 29, 247–250.

Simplício, F., Basilici, G., 2015. Unusual thick aeolian sand sheet sedimentary succession: Paleoproterozoic Bandeirinha Formation, Minas Gerais. Brazilian Journal of Geology 45, 3-11.

Simpson, E.L., Heness, E., Bumby, A., Eriksson, P.G., Eriksson, K.A., Hilbert-Wolf, H.L., Linnevelt, S. Malenda, H.F., Modungwa, T., Okafor, O.J., 2013. Evidence for 2.0 Ga continental microbial mats in a paleodesert setting. Precambrian Research, 237, 36–50.

Smoot, J.P., Castens-Seidell, B., 1994. Sedimentary features produced by efflorescent crusts, Saline Valley and Death Valley, California. In: Renaut, R.W., Last, W.M. (Eds.) Sedimentology and Geochemistry of Modern Ancient Saline Lakes. Spec. Publ. Soc. Econ. Paleont. Miner., Tulsa 50, 73-90.

Tanner, W. F., 1967. Ripple mark indices and their uses. Sedimentology 9, 89-104.

Tapias G. J., Schobbenhaus, C., 2019. Geological map of South America. Scale 1:5000000. Servicio Geologico Colombiano and CPRM Serviço Geológico do Brasil.

Taylor, I., Middleton, G.V., 1990. Aeolian sandstones in the Copper Harbor Formation, Late Proterozoic, Lake Superior basin. Canadian Journal of Earth Science 27, 1339-1347.

Tirsgaard, H., Øxnevad, I.E.I., 1998. Preservation of pre-vegetational mixed fluvio-aeolian deposits in a humid climatic setting: an example from the Middle Proterozoic Eriksfjord Formation, Southwest Greenland. Sedimentary Geology 120, 295-317.

Walden, J. White, K., Drake, N.A., 1996. Controls on dune colour in the Namib sand sea: preliminary results. Journal of African Earth Sciences 22, 349-353.

Wilson, I.G., 1973. Ergs. Sedimentary Geology 10, 77-106.

CAPTIONS

Figure 1. Current models of accumulation in (A) dry and (B) wet aeolian systems. Modified from Mountney (2012).

Figure 2. (A) Geographical and large-scale geological map of the study area. Modified by Santos et al. (2015) and Tapias and Schobbenhaus (2019). (B) Detailed map of the study area. The circles indicate the interpreted depositional aeolian subenvironments. Modified from CODEMIG (2012a, 2012b). (C) Overall lithostratigraphy of the Espinhaço Supergroup exposed in study and neighbouring areas. Modified by Santos et al. (2015).

Figure 3. Compound sets of cross-strata (draas), large-scale simple sets of cross strata (large-scale isolated simple dunes) and planar-parallel sandstone strata (dry interdraas or interdunes) architectural elements. Locality: Serra do Pasmar, southern sector of the study area. The three images represent (A) the original picture, (B) the identifications by field drawings and photomosaic of the bounding surfaces and (C) the architectural interpretative sketch. The foreset dip-azimuths showed in the panel use a rose diagram oriented relative to the face of the observer; see the small circle at the bottom for azimuth values. Small north-oriented rose diagram to the left indicate the dip-azimuths of the foresets of cross-strata. See text for description and discussion.

Figure 4. Compound sets of cross-strata (draas), large-scale simple sets of cross strata (large-scale isolated simple dunes) and planar-parallel sandstone strata (dry interdraas or interdunes) architectural elements. Locality: Morro Batatal South, south portion of the study area. The three images represent (A) the original picture, (B) the identifications by field drawings and photomosaic of the bounding surfaces and (C) the architectural interpretative sketch. The foreset dip-azimuths showed in the panel use a rose diagram oriented relative to the face of the observer; see the small circle at the bottom for azimuth values. Small north-oriented rose diagram to the left and right indicate the dip-azimuths of the foresets of cross-strata. See text for description and discussion.

Figure 5. (A) Stratigraphic log at locality Morro do Alojamento, northern sector of the study area. The succession is composed by the interbedding of wavy and planar-parallel bed sandstone (damp/wet sand sheet), small-scale sets of cross strata (small-scale isolated simple dunes) and compound sets of cross-strata (draas) architectural elements. This succession represents the damp/wet sand sheet subenvironment. Note that at the stratigraphic high of 5 and

7.5 m the toe of the foresets of the compound sets of cross-strata is laterally transitional to wave-rippled beds. (B) Stratigraphic log at locality Morro do Rio Preto, northern sector of the study area. Wavy and planar-parallel bed sandstone (damp/wet sand sheet) and small-scale simple sets of cross-strata (small-scale isolated simple dunes) architectural elements are captured by this stratigraphic log. This succession represents the damp/wet sand sheet subenvironment.

Figure 6. Descriptive and interpretative draft of the erosional bounding surfaces characterising the compound sets of cross-strata and the simple sets of cross-strata architectural elements.

Figure 7. Compound sets of cross-strata (draas), large- and small-scale simple sets of cross-strata (large- and small scale isolated simple dunes) and planar-parallel laminated strata (dry interdraas or interdunes) architectural elements. Locality: Morro Batatal North, south portion of the study area. The three images represent (A) the original picture, (B) the identifications by field drawings and photomosaic of the bounding surfaces and (C) the architectural interpretative sketch. The foreset dip-azimuths showed in the panel use a rose diagram oriented relative to the face of the observer; see the small circle to the right for azimuth values. Small north-oriented rose diagram to the left indicate the dip-azimuths of the foresets of cross-strata. See text for description and discussion.

Figure 8. Compound sets of cross-strata (draas) and wavy and planar-parallel bed sandstone (damp/wet sand sheet) architectural elements. Locality: Vargem do Padre 2, northern sector of the study area. The three images represent (A) the original picture, (B) the identifications by field drawings and photomosaic of the bounding surfaces and (C) the architectural interpretative sketch. The foreset dip-azimuths showed in the panel use a rose diagram oriented relative to the face of the observer; see the small circle at the bottom for azimuth values. Small north-oriented

rose diagram indicate the dip-azimuths of the foresets of cross-strata. See text for description and discussion.

Figure 9. Locality Morro do Alojamento (north of study area). An element of compound sets of cross-strata, ca. 3 m thick, displays a convex-up top surface onlapped at the margins by wavy and planar-parallel bed sandstone. This atypical erosional top surface is attributed to the adhesive action of the capillary fringe of the groundwater that hindered the erosion of sand by the wind.

Figure 10. (A) Stratigraphic log at locality Morro Batatal north, southern sector of the study area. The succession is composed by the interbedding of compound sets of cross-strata and planar-parallel sandstone beds. This succession is constituted of draas deposits interbedded with interdraa deposits in a general dry subenvironment. Some interbedding of vortex-rippled beds suggests oscillation of the groundwater table near to the depositional surface. This section was measured 150 m to west of the section represented in Figure 5. (B) Stratigraphic log at locality Morro do Pasmar East, south portion of the study area. The succession is composed by the interbedding of large-scale simple set of cross-strata and planar-parallel sandstone beds. This succession is deposited in a subenvironment characterised by isolated large-scale dunes and dry interdune area. Some beds of vortex ripples indicate temporary oscillations of the groundwater level above the depositional surfaces. This section was measured in the exposure showed in Figure 9.

Figure 11. Summary of stratigraphic description and morphological interpretation of compound sets of cross-strata, large-scale simple sets of cross-strata and planar-parallel sandstone strata. These architectural elements represent a subenvironment characterised for

draas, dry interdraas and large-scale isolated simple dunes. The depositional surface was dry, but the groundwater level is assumed to be located a few metres below this surface, thus influencing the accumulation and preservation of these bedforms.

Figure 12. Large and small-scale simple sets of cross-strata (large- and small scale isolated simple dunes) alternated with the architectural type planar-parallel laminated strata (dry interdunes). Locality: Serra do Pasmar, southern sector of the study area. The three images represent (A) the original picture, (B) the identifications by field drawings and photomosaic of the bounding surfaces and (C) the architectural interpretative sketch. The foreset dip-azimuths showed in the panel use a rose diagram oriented relative to the face of the observer; see the small circle to the left for azimuth values. Small north-oriented rose diagram indicated the dip-azimuths of the foresets of cross-strata. See text for description and discussion.

Figure 13. (A) Fourth order erosional surfaces (dashed line in this picture) attributed to reactivation surface in large-scale sets of cross-strata. Morro Batatal North. Hammer: 0.28 m. (B) Transitional contact between the toes of the cross-strata and planar-parallel laminations (see arrows). The picture is a detail of Figure 3. (C) Small-scale simple sets of cross-strata commonly show downdip lateral transition of the toes of the foresets to vortex-rippled beds (arrows). The arrows indicate the height of 14 m of the section in Figure 4A. (D) The top surfaces of small-scale simple cross-strata is commonly characterised by erosional steps and depressions associated with differential erosion by wind in damp sand. Locality: Laje da Doida, see Fig. 2B. (E) Sometimes small-scale simple cross-strata are characterised by soft deformation, consisting in small narrow anticline and wider syncline folds. Locality: Tromba d'Anta. Hammer: 0,28 m. (F) and (G) Rose diagram of the foreset dip azimuths of large- and small-scale simple sets of cross-strata. (H) Planar-parallel bed sandstone consists in planar or very low-angle laminations

attributed to the deposition of wind ripples. In this picture planar-parallel laminations erosively overlay large-scale simple cross-strata. Hammer: 0.28 m.

Figure 14. Small-scale simple sets of cross-strata (large- and small scale isolated simple dunes) and wavy and planar-parallel bed sandstone (damp wet sand sheet) architectural elements. Locality: Morro Redondo, northern sector of the study area. The three images represent (A) the original picture, (B) the identifications by field drawings and photomosaic of the bounding surfaces and (C) the architectural interpretative sketch. The foreset dip-azimuths showed in the panel use a rose diagram oriented relative to the face of the observer; see the small circle to the right for azimuth values. See text for description and discussion.

Figure 15. Summary of stratigraphic description and morphological interpretation of large-scale simple sets of cross-strata and planar-parallel sandstone strata. This depositional subenvironment consisted of large-scale dunes separated by extensive dry interdune areas. Yet, some interbeddings of vortex-rippled beds testify to a groundwater level a few meters from the depositional surface. This subenvironment is more common in the southern and central portions of the study area (Fig. 2B).

Figure 16. Summary of stratigraphic description and morphological interpretation of wavy and planar-parallel bed sandstone, small-scale simple sets of cross-strata and irregular horizontal beds. This subenvironment was dominated by a damp/wet sand sheet with isolated small simple dunes and localised salt flat. Groundwater level was located near or above the depositional surface. This subenvironment represents most of the Galho do Miguel Formation and it is dominant in central and northern part of the study area.

Figure 17. Microphotograph of an inverse grading lamina of planar-parallel sandstone strata. This microstructure, the geometry of these strata and the relationship with the other lithofacies suggest they are formed by deposition of climbing wind ripples.

Figure 18. Wavy and planar-parallel bed sandstone architectural element. (A) The lenticular bed indicated by the arrow has concave-up erosional bottom and it is filled by wave-rippled sandstone. It represents the subaqueous filling of a small hollow. Morro Redondo, northern sector of the study area. The subdivisions of the Jacob's staff are 0.1 m. (B) Vortex ripple bedforms on the bed surfaces. The rounded crest is attributed to reworking of the waves during the lowering of the water level. Coin: 20 mm in diameter. Morro do Rio Preto, northern part of study area. (C) Climbing vortex ripples in vertical section. The high climbing angle means a high input of sediment in wavy water, probably carried by wind. Morro do Alojamento, northern sector of the study area. (D) Small asymmetrical microridges (1 mm high and spaced 4 mm) on bedding surfaces correspond to adhesion ripples formed by wind transported sand on a damp depositional surfaces. Coin: 20 mm in diameter. Morro Redondo, northern part of the study area. (E) Adhesion ripples in vertical section show undulating and irregular pseudo-cross-laminations inclined up to 45°. Notice the undulated adhesion ripple bedforms indicated by the arrow at the top of the bed. Coin: 20 mm in diameter. Morro do Rio Preto, northern sector of the study area.

Figure 19. Irregular horizontal beds. (A) This architectural element consists in thin discontinuous white bed of very fine- and fine-grained sandstone layers (yellow arrow) alternating with light-grey muddy very fine-grained sandstone layers (black arrow). White layer can be subdivided in six types. All these sedimentary structures can be attribute to interaction of precipitation of efflorescence crusts of evaporite minerals and various depositional processes; see the text for the interpretation. (B) A first type is constituted of small patches of white

sandstone with jagged and cuspate boundaries (yellow arrow) and bottom characterised of small protrusion of light-grey muddy sandstone (black arrow). (C) Concave-up lens of white sandstone with narrow anticline and wider syncline; sometime the anticline's hinge is broken (yellow arrow). (D) Concave-up lens of white sandstone can display a vertical superposition, like a pile of dishes. Hammer: 0.28 m long. (E) Isolated lens of white sandstone (yellow arrow) with pronounced concave-up bottom, apparently filling a depression. Coin: 20 mm in diameter. (F) Isolated lens white sandstone that partially fill a concave-up erosive small depression. Notice the erosion of previous thin layers (yellow arrow). (G) Small and regularly spaced convex-up white sandstone on the depositional surface. (H) Vertical section of climbing vortex ripples.

Figure 20. (A) Vortex ripples passing laterally on the same bedding surface to smooth areas (black arrow). Linear and anastomosed cracks cross the rippled and the smooth surface (yellow arrow). (B) Linear and anastomosed cracks are in general developed on the crests of the ripples, but sometime cross the ripple troughs and form polygonal cracks. See the text for the interpretation.

Figure 21. The groundwater level controlled the construction of the four depositional subenvironments. Although dry subenvironments prevail in the southern sector of the study area and damp/wet subenvironment prevail in the central and northern parts, local transitions between these subenvironments can be observed throughout the investigated area.

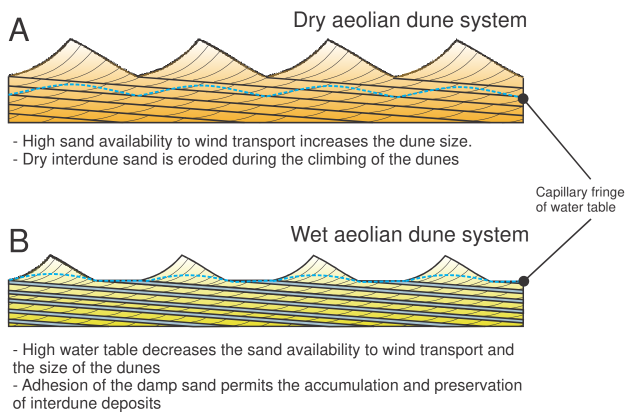
A
Dry aeolian dune system
- High sand availability to wind transport increases the dune size.
- Dry interdune sand is eroded during the climbing of the dunes
Capillary fringe
of water table
B
Wet aeolian dune system
- High water table decreases the sand availability to wind transport and the size of the dunes
- Adhesion of the damp sand permits the accumulation and preservation of interdune deposits

FIGURE 1

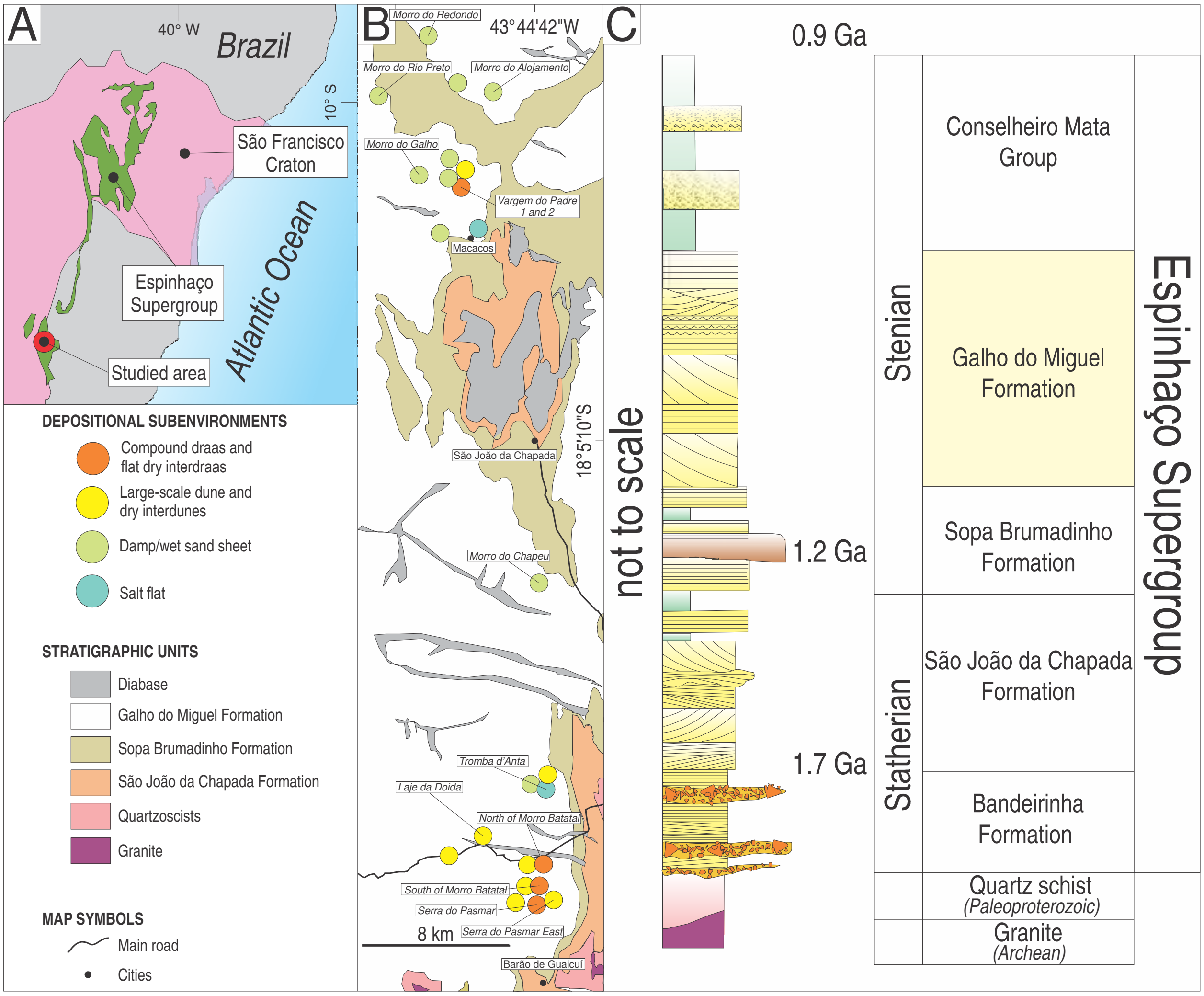
A
40° W
Brazil
10° S
São Francisco Craton
Espinhaço Supergroup
Atlantic Ocean
Studied area
DEPOSITIONAL SUBENVIRONMENTS
Compound draas and flat dry interdraas
Large-scale dune and dry interdunes
Damp/wet sand sheet
Salt flat
STRATIGRAPHIC UNITS
Diabase
Galho do Miguel Formation
Sopa Brumadinho Formation
São João da Chapada Formation
Quartzoscists
Granite
MAP SYMBOLS
Main road
Cities
B
43°44'42"W
Morro do Redondo
Morro do Rio Preto
Morro do Alojamento
Morro do Galho
Vargem do Padre 1 and 2
Macacos
São João da Chapada
18°5'10"S
Morro do Chapeu
Tromba d'Anta
Laje da Doida
North of Morro Batatal
South of Morro Batatal
Serra do Pasmar
Serra do Pasmar East
8 km
Barão de Guaicuí
C
not to scale
0.9 Ga
1.2 Ga
1.7 Ga
Stenian
Statherian
Conselheiro Mata Group
Galho do Miguel Formation
Sopa Brumadinho Formation
São João da Chapada Formation
Bandeirinha Formation
Quartz schist
(Paleoproterozoic)
Granite
(Archean)
Espinhaço Supergroup

FIGURE 2

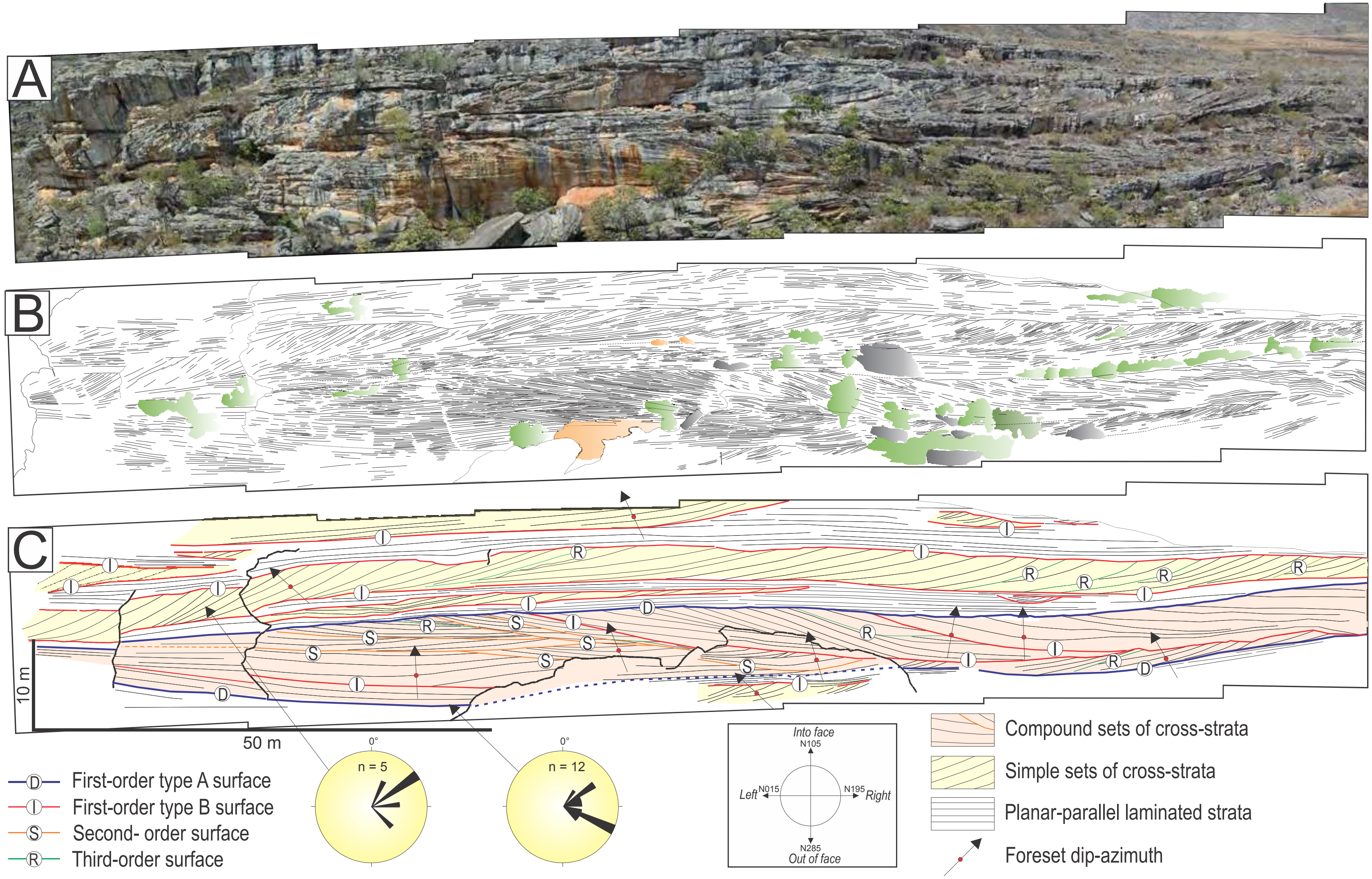
A
B
C
10 m
50 m
First-order type A surface
First-order type B surface
Second- order surface
Third-order surface
n = 5
n = 12
Into face
N105
Left
N015
N195
Right
N285
Out of face
Compound sets of cross-strata
Simple sets of cross-strata
Planar-parallel laminated strata
Foreset dip-azimuth

FIGURE 3

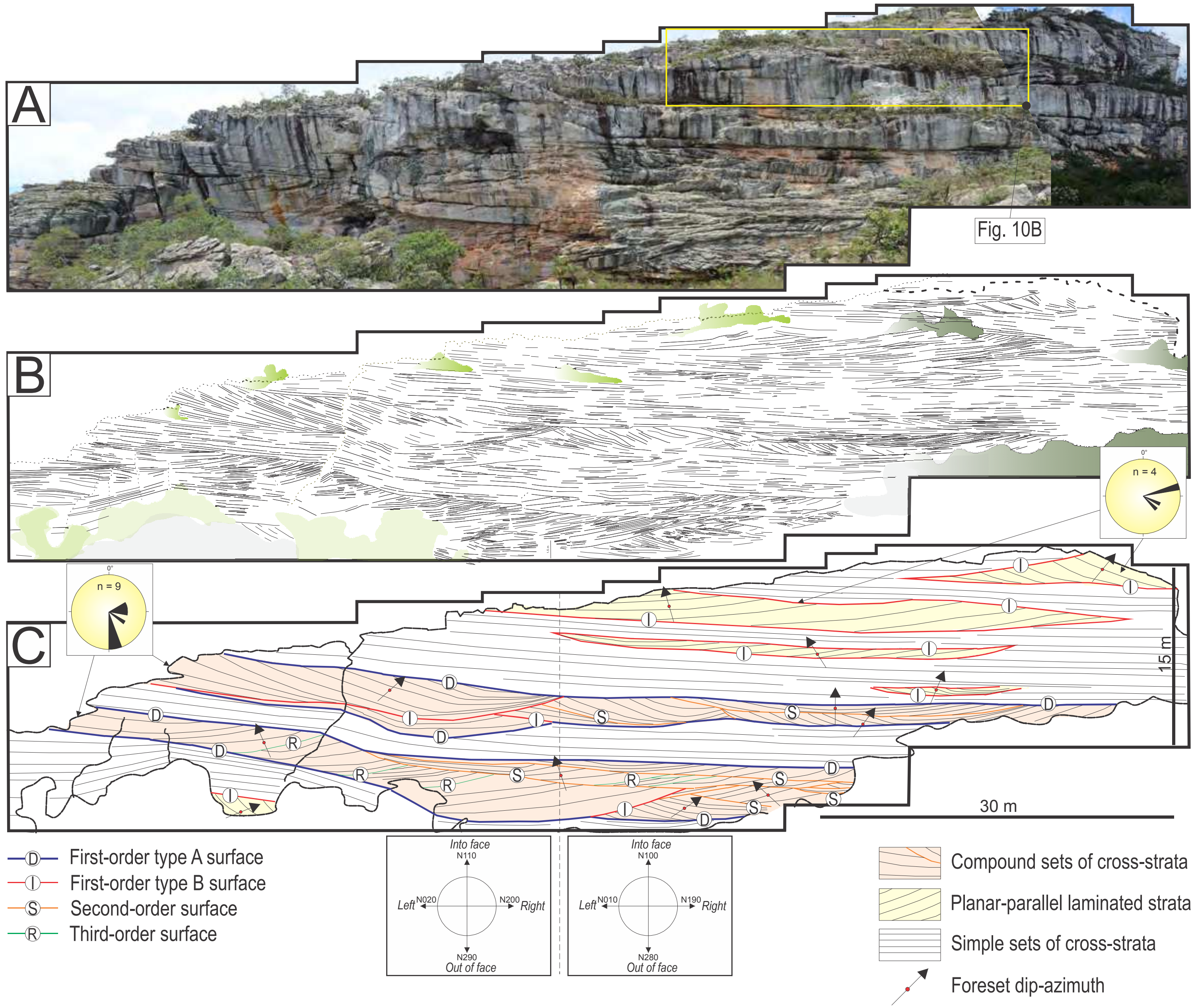

A
Fig. 10B
B
n = 4
C
n = 9
15 m
30 m
First-order type A surface
First-order type B surface
Second-order surface
Third-order surface
Into face
N110
Left N020
N200 Right
N290
Out of face
Into face
N100
Left N010
N190 Right
N280
Out of face
Compound sets of cross-strata
Planar-parallel laminated strata
Simple sets of cross-strata
Foreset dip-azimuth

FIGURE 4

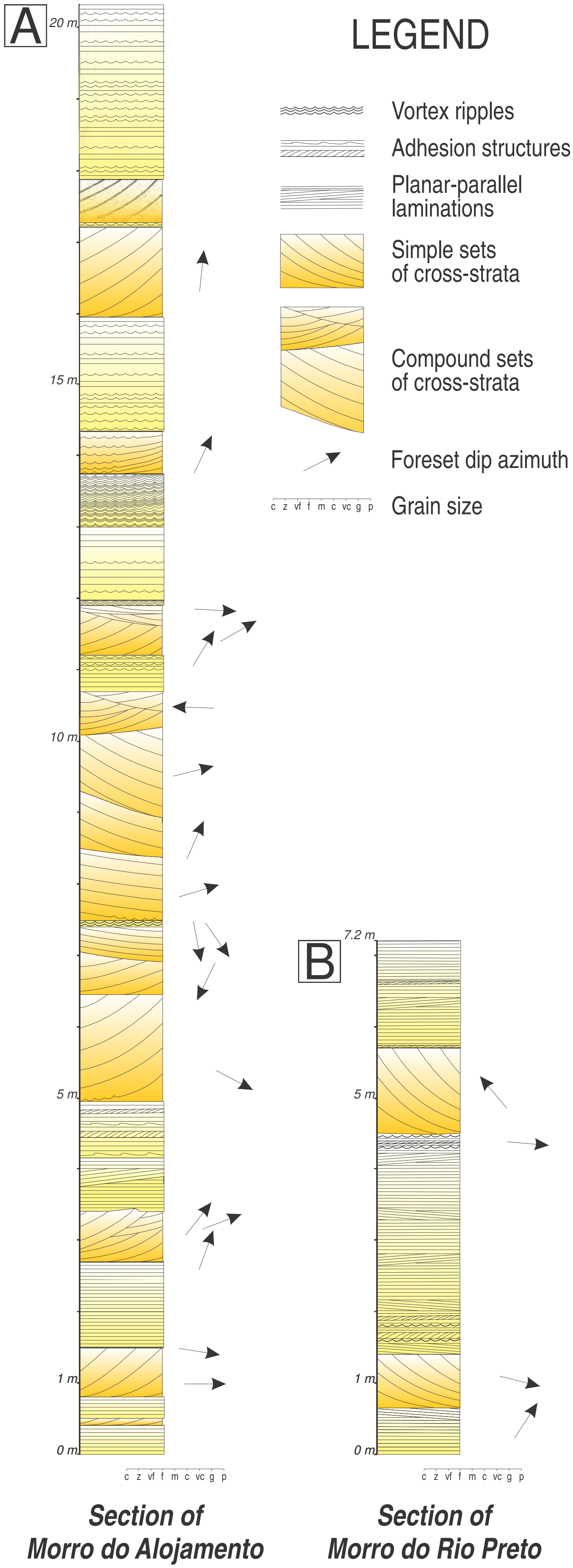
A
LEGEND
Vortex ripples
Adhesion structures
Planar-parallel laminations
Simple sets of cross-strata
Compound sets of cross-strata
Foreset dip azimuth
Grain size
c z vf f m c vc g p
20 m
15 m
10 m
5 m
1 m
0 m
B
7.2 m
Section of Morro do Alojamento
Section of Morro do Rio Preto

FIGURE 5

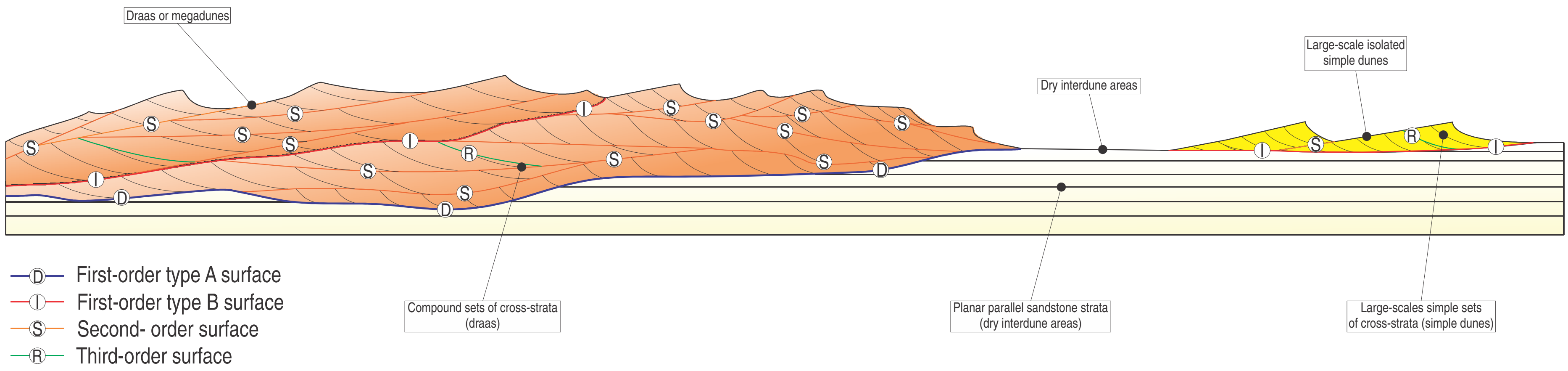

Draas or megadunes
Large-scale isolated simple dunes
Dry interdune areas
First-order type A surface
First-order type B surface
Second- order surface
Third-order surface
Compound sets of cross-strata (draas)
Planar parallel sandstone strata (dry interdune areas)
Large-scales simple sets of cross-strata (simple dunes)

FIGURE 6

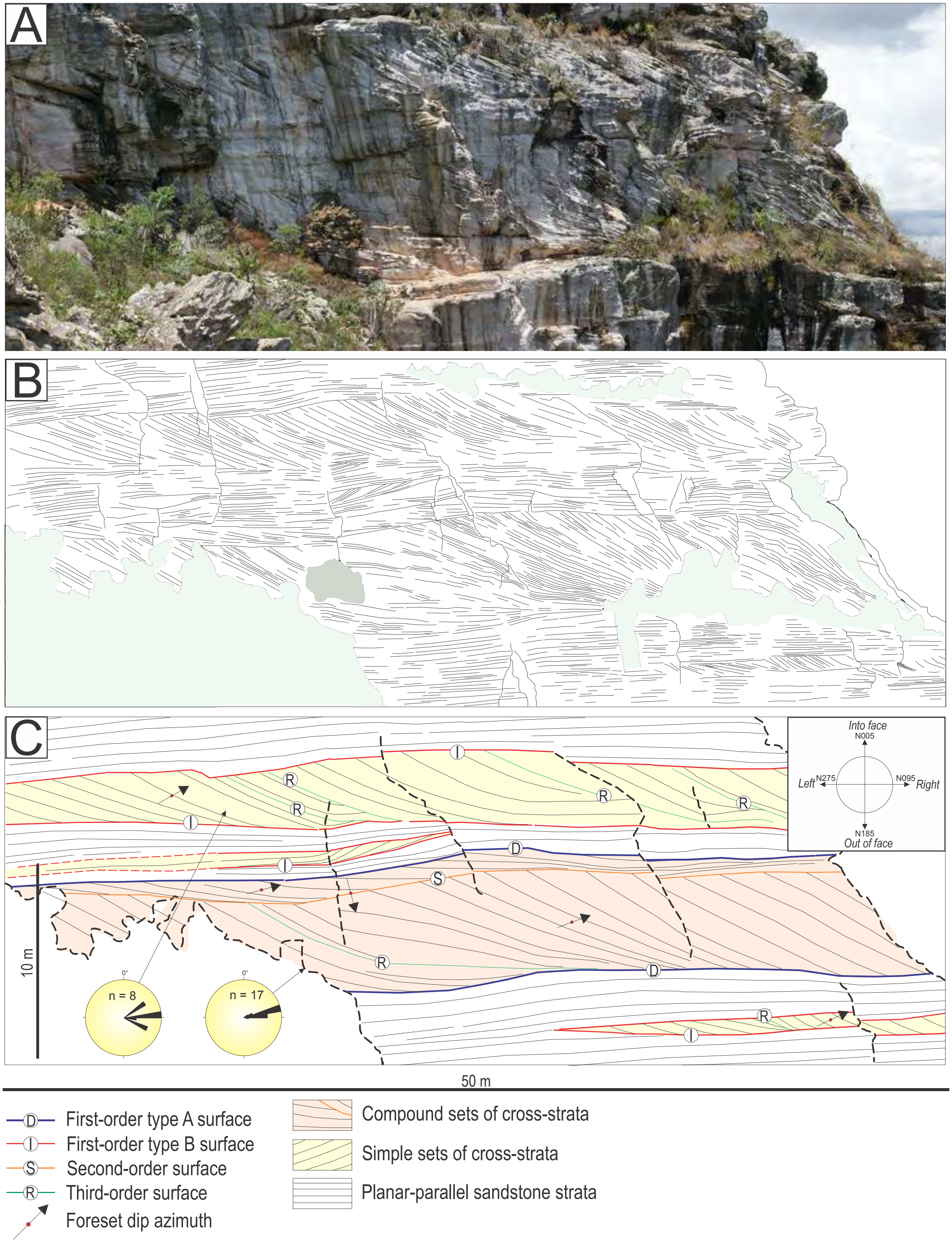
A
B
C
Into face
N005
Left
N275
N095
Right
N185
Out of face
10 m
n = 8
n = 17
50 m
First-order type A surface
First-order type B surface
Second-order surface
Third-order surface
Foreset dip azimuth
Compound sets of cross-strata
Simple sets of cross-strata
Planar-parallel sandstone strata

FIGURE 7

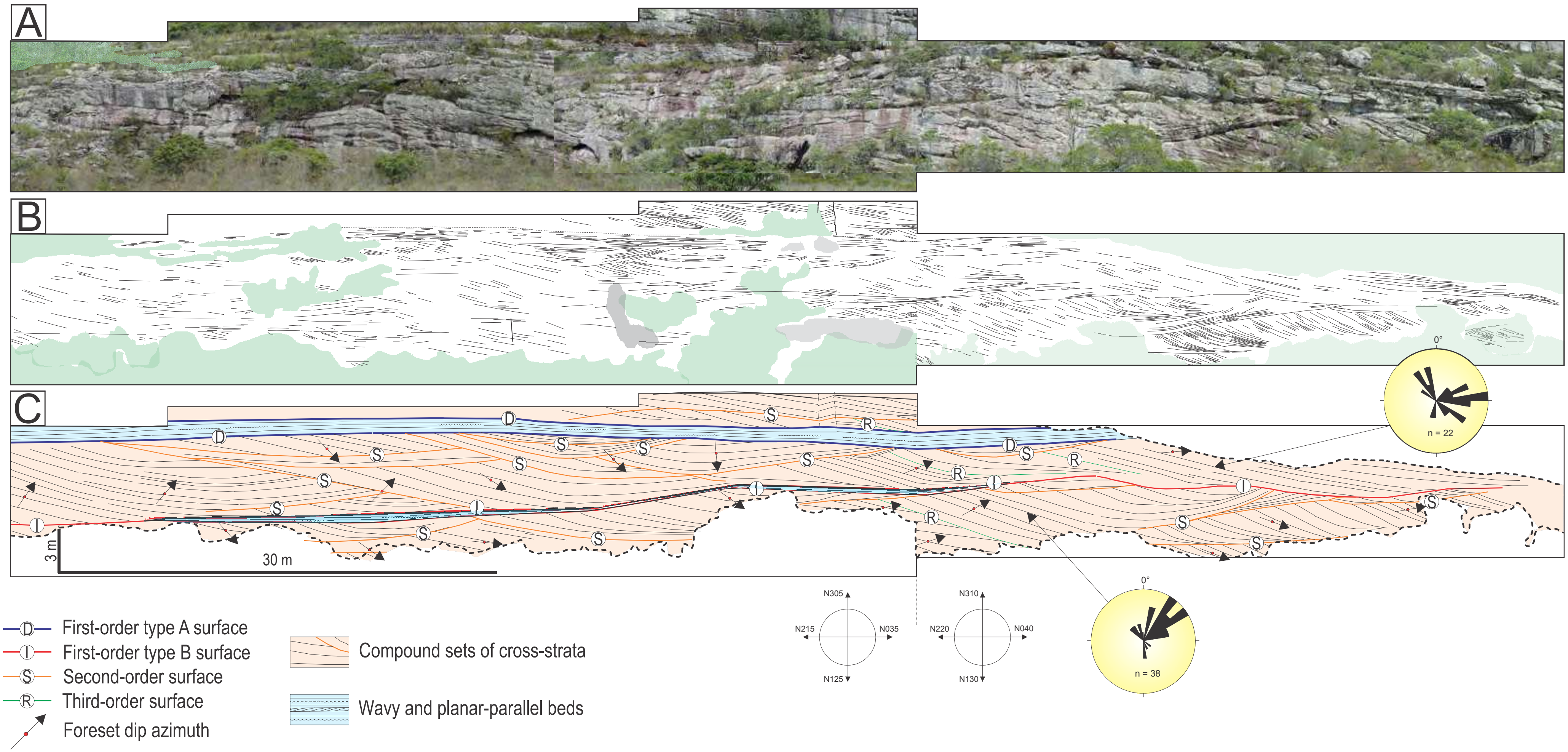
A
B
C
3 m
30 m
0°
n = 22
n = 38
N305
N215
N035
N125
N310
N220
N040
N130
First-order type A surface
First-order type B surface
Second-order surface
Third-order surface
Foreset dip azimuth
Compound sets of cross-strata
Wavy and planar-parallel beds

FIGURA 8

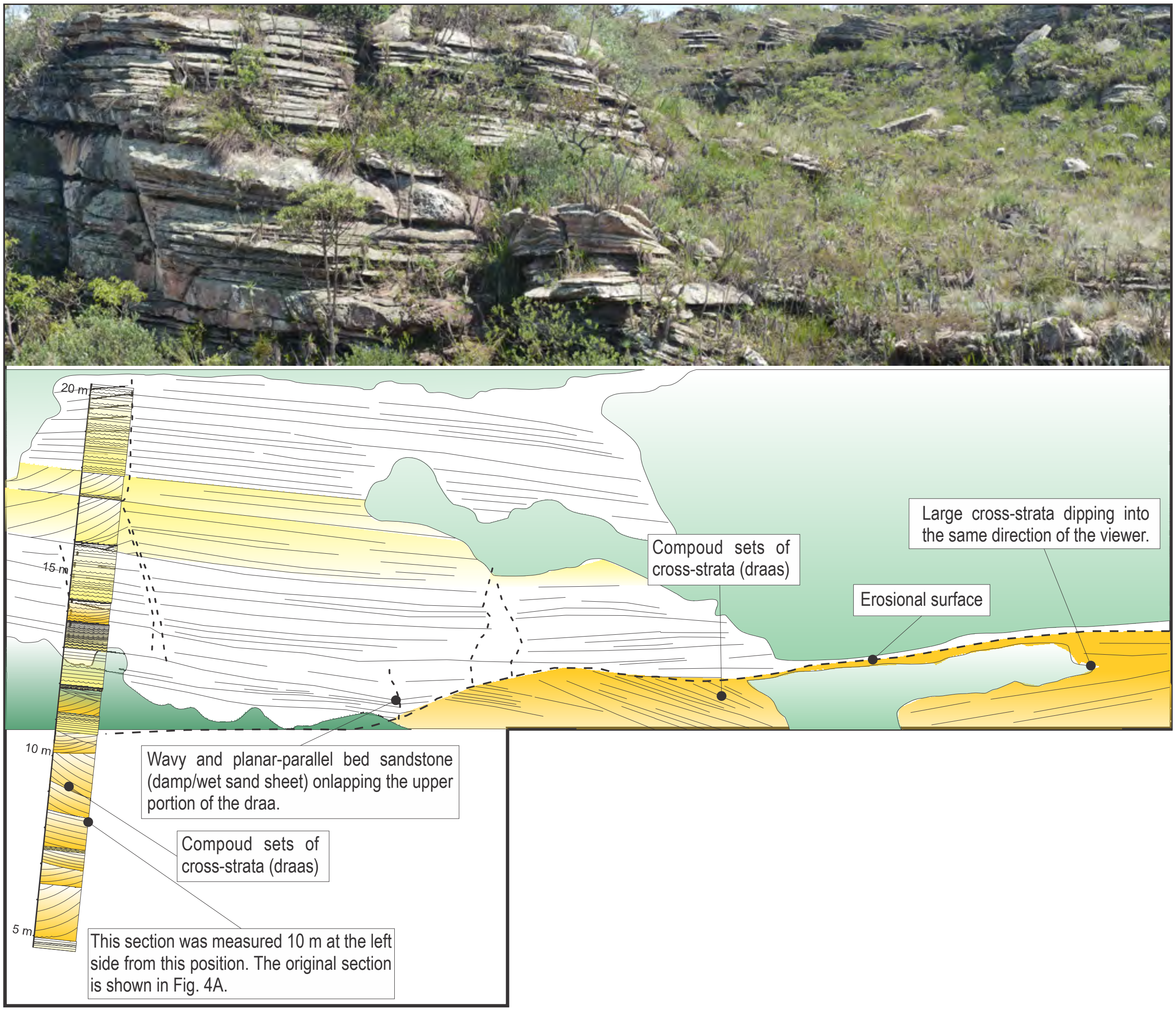
20 m
15 m
10 m
5 m
Large cross-strata dipping into the same direction of the viewer.
Compound sets of cross-strata (draas)
Erosional surface
Wavy and planar-parallel bed sandstone (damp/wet sand sheet) onlapping the upper portion of the draa.
Compound sets of cross-strata (draas)
This section was measured 10 m at the left side from this position. The original section is shown in Fig. 4A.

FIGURE 9

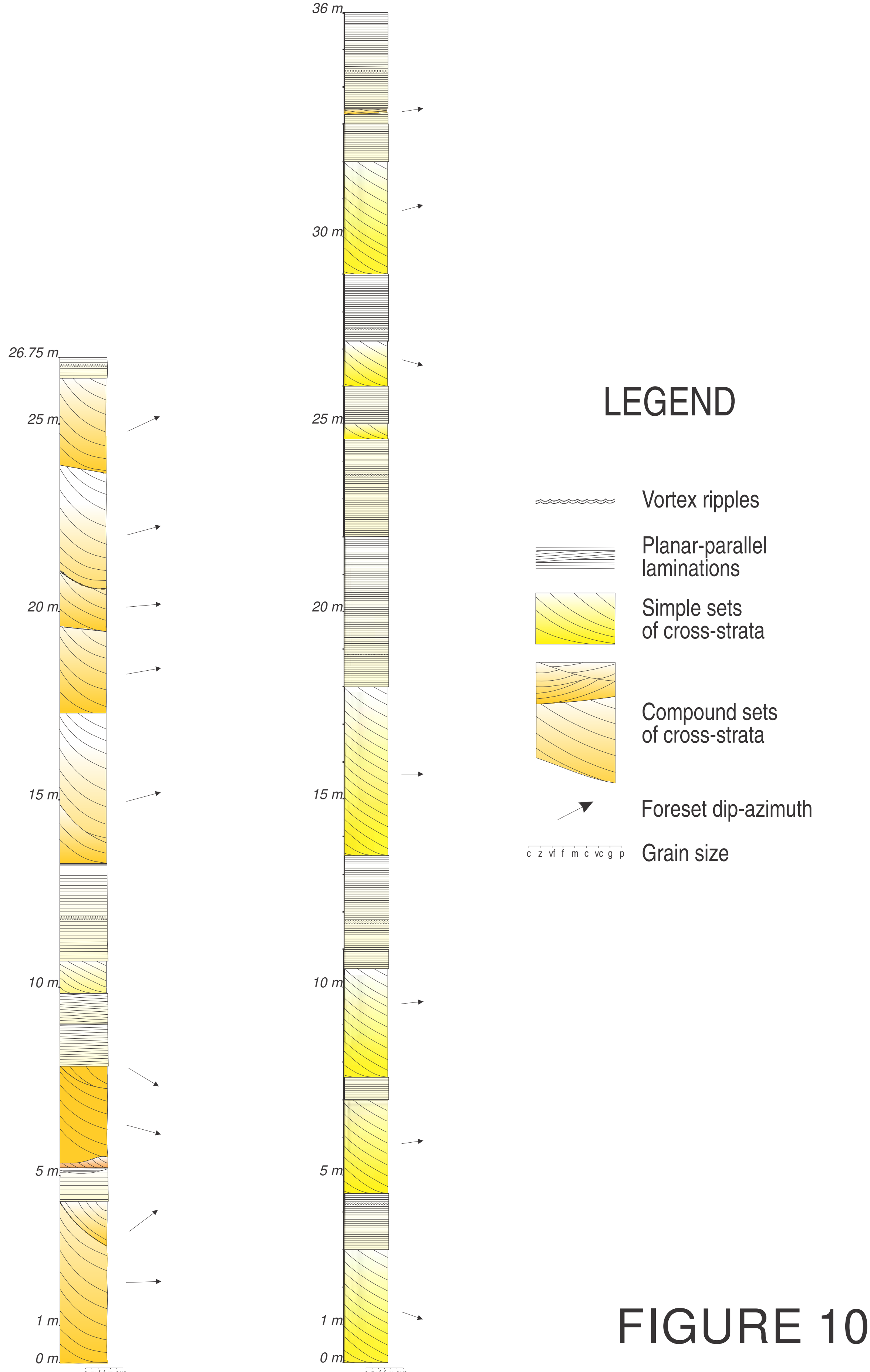

FIGURE 10

Section of Morro Batatal North

Section of Serra do Pasmar East

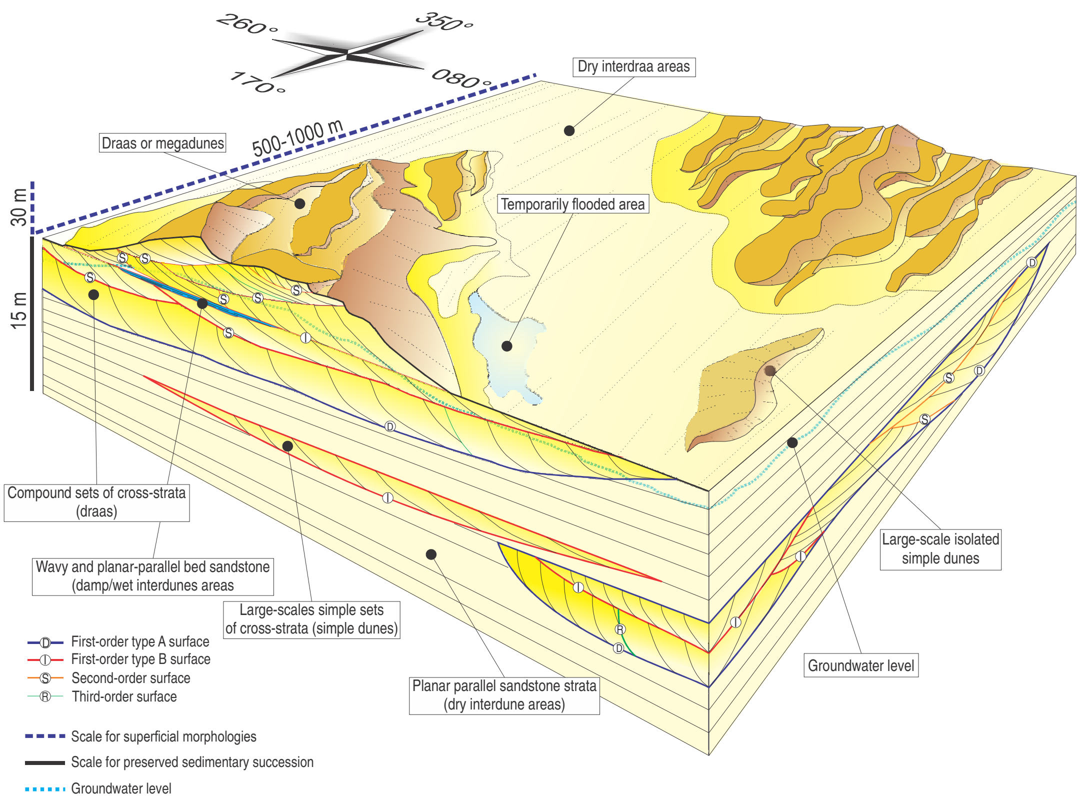
260°
350°
170°
080°
Dry interdraa areas
500-1000 m
Draas or megadunes
30 m
15 m
Temporarily flooded area
Compound sets of cross-strata (draas)
Wavy and planar-parallel bed sandstone (damp/wet interdunes areas)
Large-scales simple sets of cross-strata (simple dunes)
Planar parallel sandstone strata (dry interdune areas)
Large-scale isolated simple dunes
Groundwater level
First-order type A surface
First-order type B surface
Second-order surface
Third-order surface
Scale for superficial morphologies
Scale for preserved sedimentary succession
Groundwater level

FIGURE 11

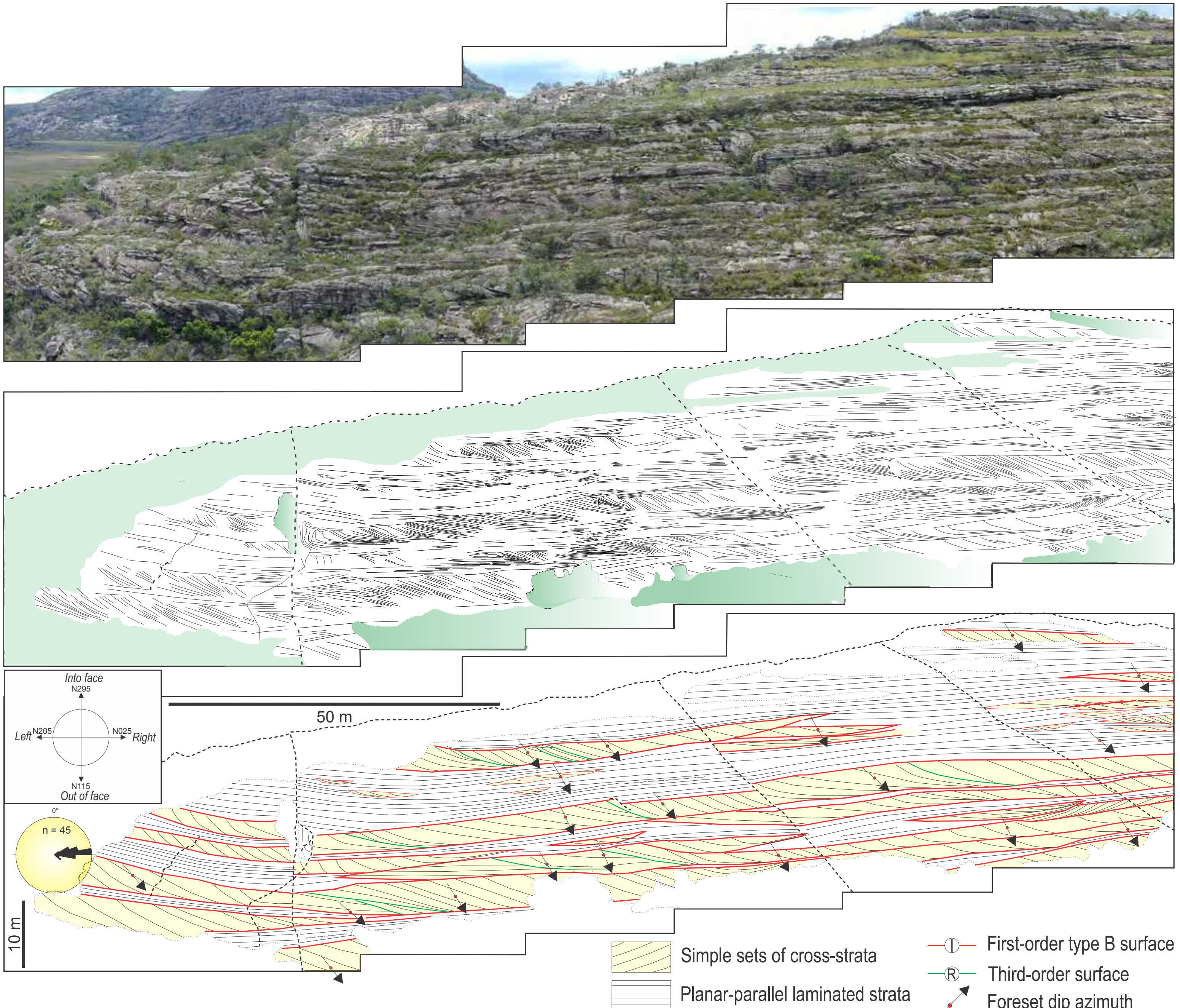

Into face
N295
Left
N205
N025
Right
N115
Out of face
0°
n = 45
50 m
10 m
Simple sets of cross-strata
Planar-parallel laminated strata
First-order type B surface
Third-order surface
Foreset dip azimuth

FIGURE 12

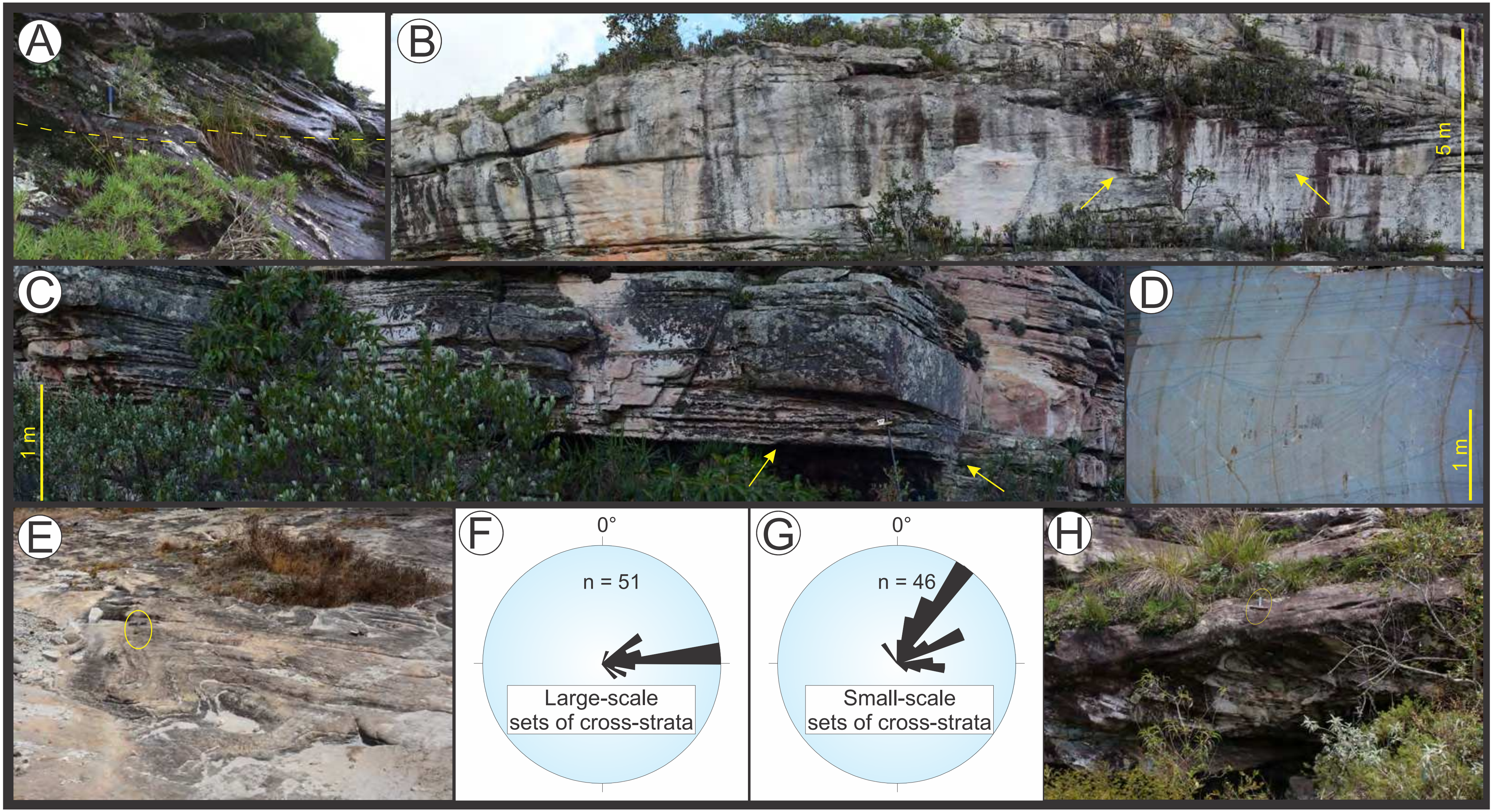
A
B
5 m
C
1 m
D
1 m
E
F
0°
n = 51
Large-scale
sets of cross-strata
G
0°
n = 46
Small-scale
sets of cross-strata
H

FIGURE 13

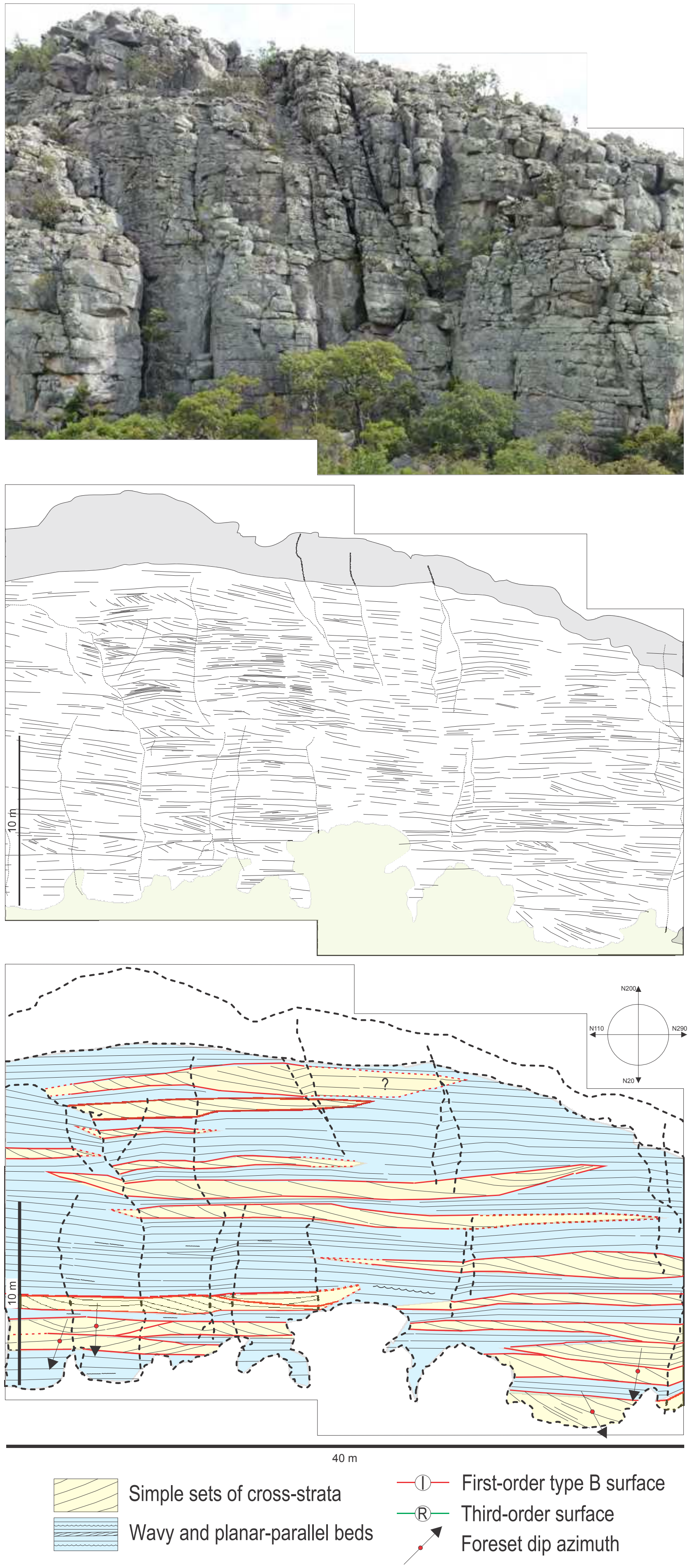

10 m
?
N200
N110
N290
N20
10 m
40 m
Simple sets of cross-strata
Wavy and planar-parallel beds
First-order type B surface
Third-order surface
Foreset dip azimuth

FIGURE 14

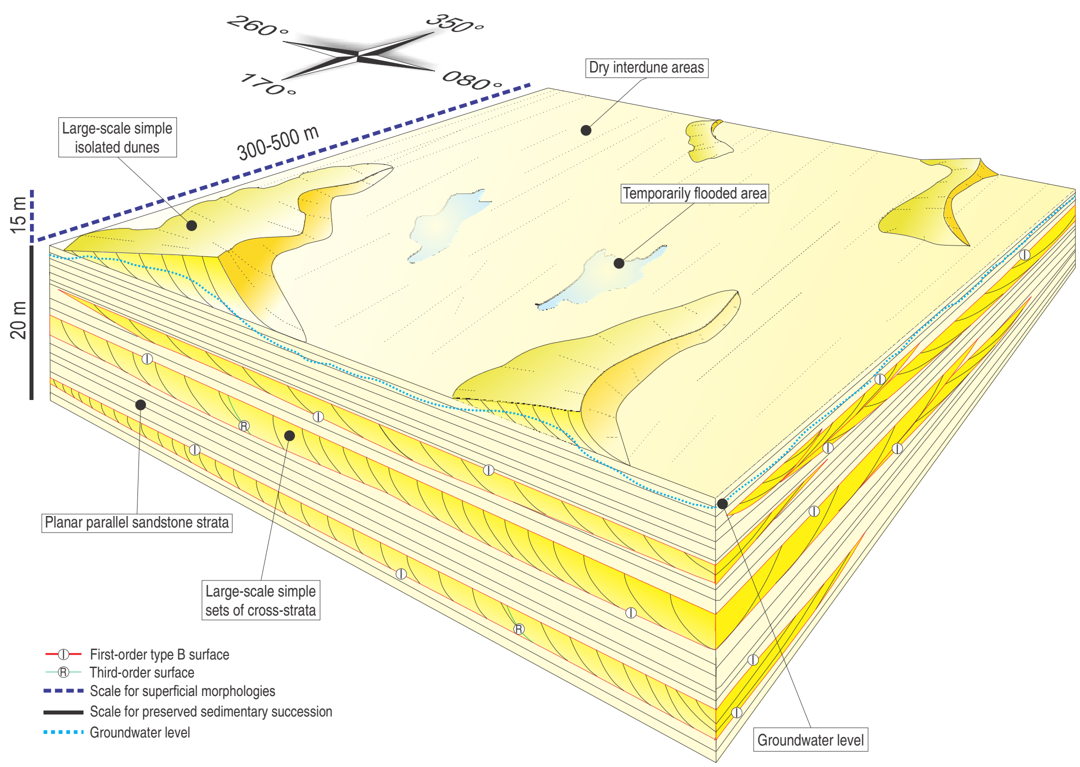

260°
350°
170°
080°
300-500 m
15 m
20 m
Dry interdune areas
Large-scale simple isolated dunes
Temporarily flooded area
Planar parallel sandstone strata
Large-scale simple sets of cross-strata
Groundwater level
First-order type B surface
Third-order surface
Scale for superficial morphologies
Scale for preserved sedimentary succession
Groundwater level

FIGURE 15

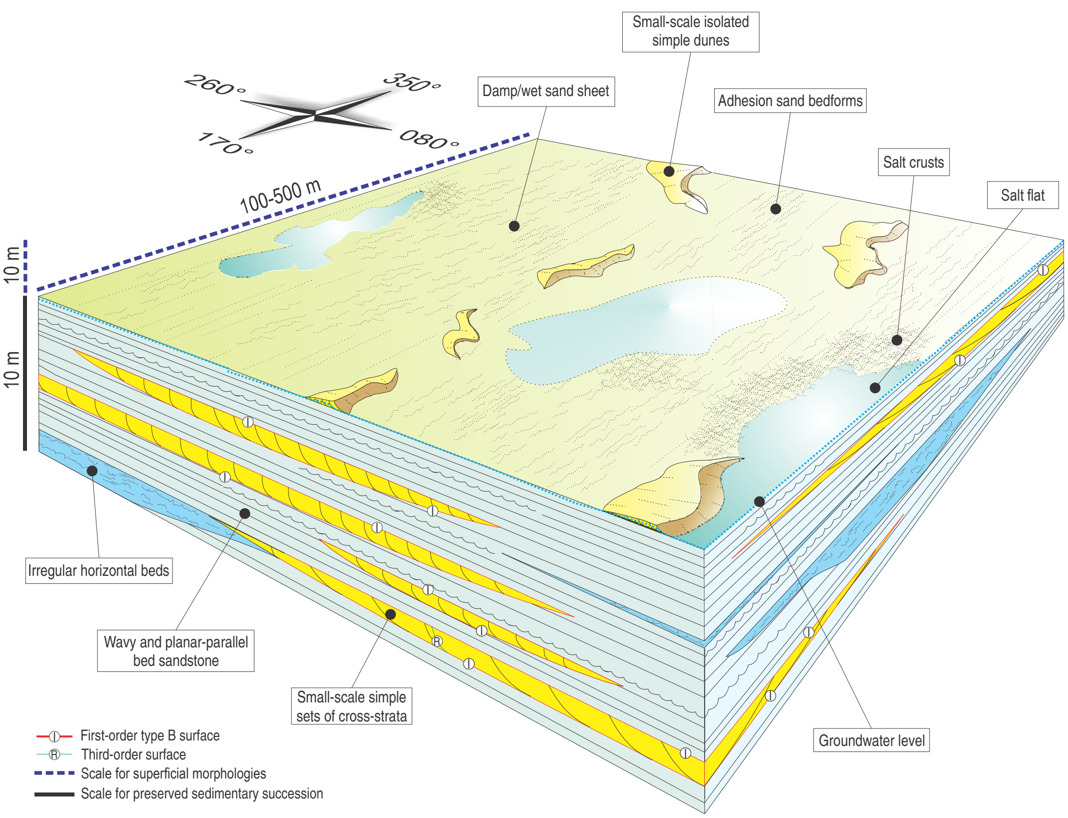

260°
350°
170°
080°
100-500 m
10 m
10 m
Damp/wet sand sheet
Small-scale isolated simple dunes
Adhesion sand bedforms
Salt crusts
Salt flat
Irregular horizontal beds
Wavy and planar-parallel bed sandstone
Small-scale simple sets of cross-strata
Groundwater level
First-order type B surface
Third-order surface
Scale for superficial morphologies
Scale for preserved sedimentary succession

FIGURE 16

FIGURE 17

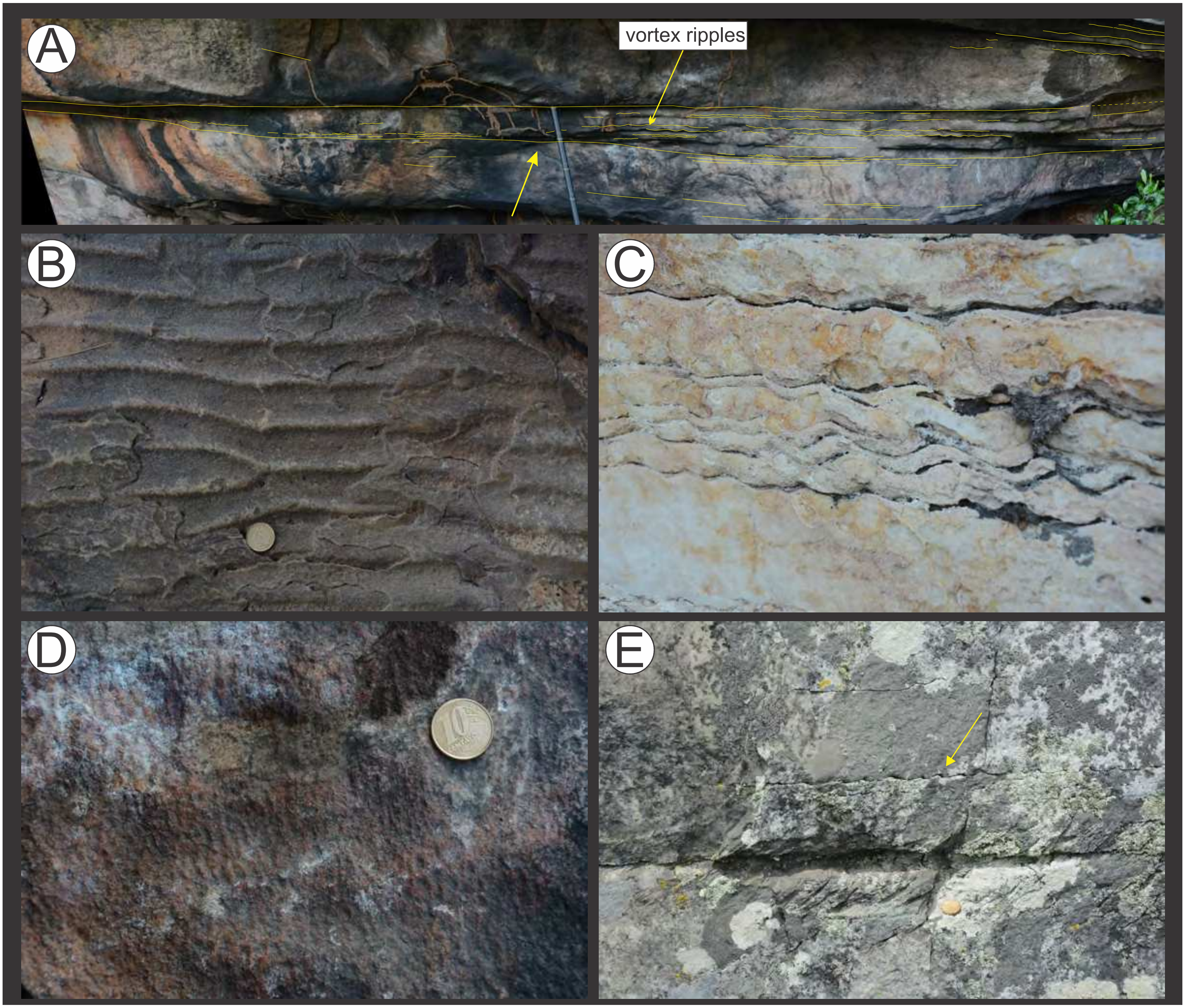

FIGURE 18

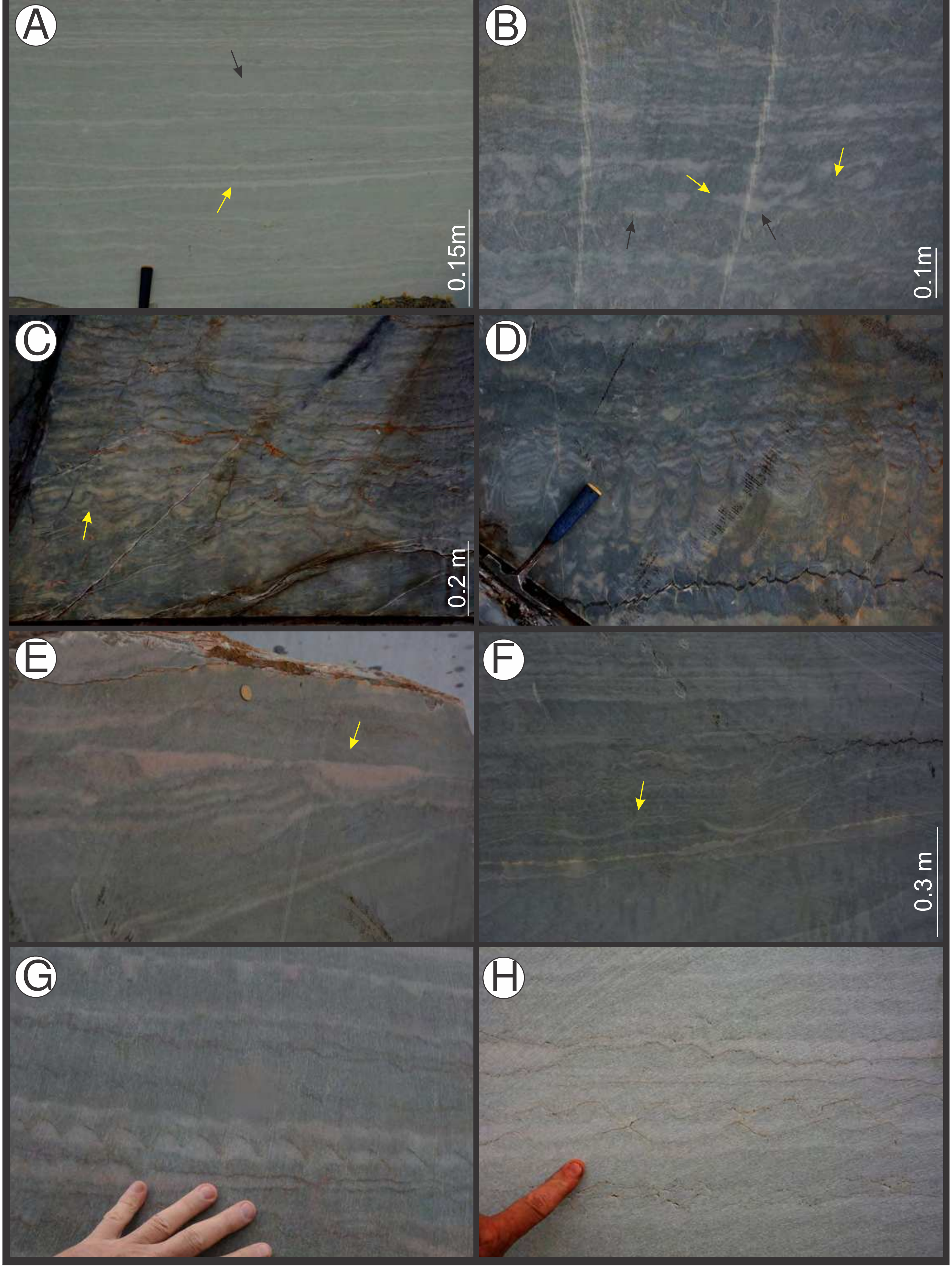

FIGURE 19

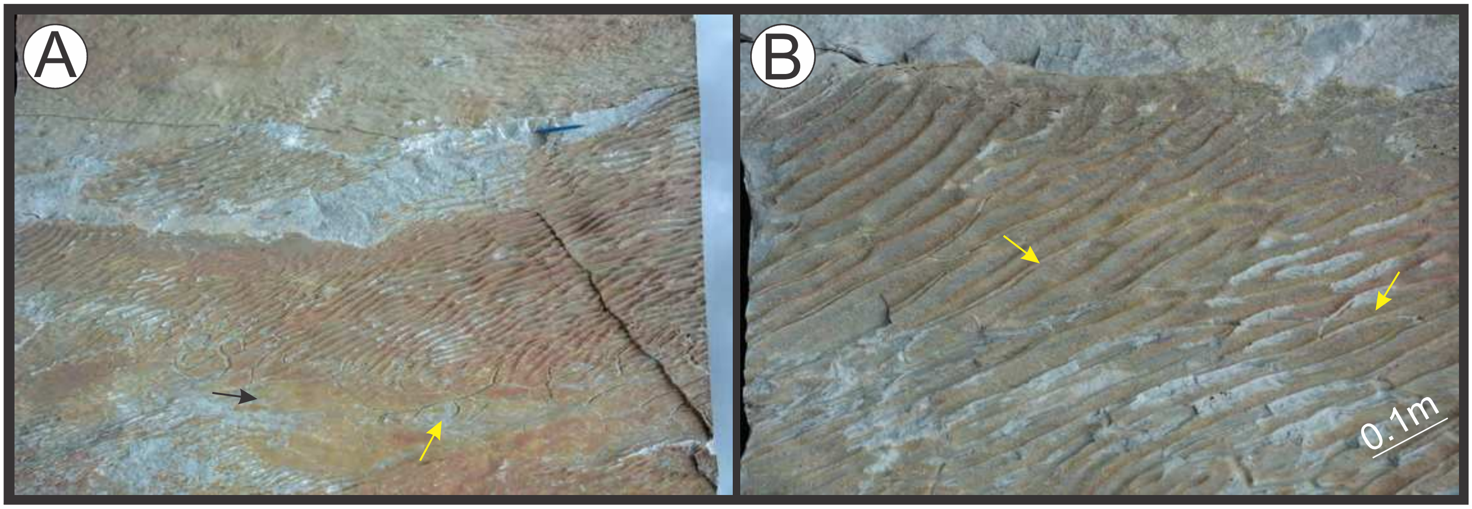

FIGURE 20

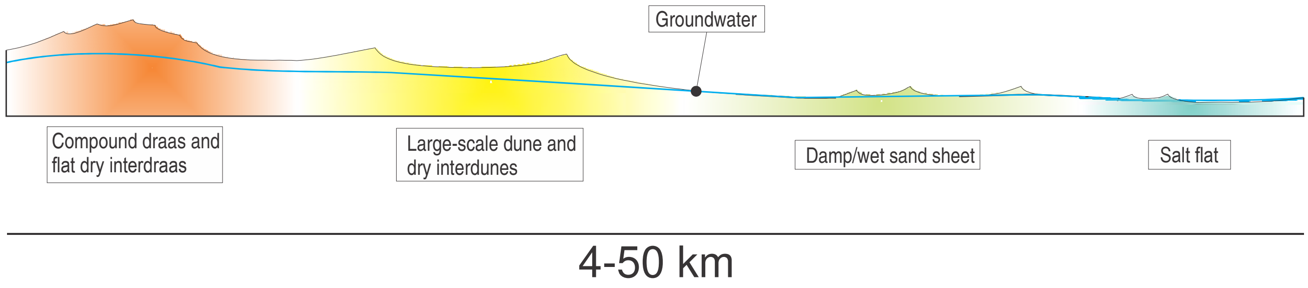
Groundwater
Compound draas and
flat dry interdraas
Large-scale dune and
dry interdunes
Damp/wet sand sheet
Salt flat
4-50 km

FIGURE 21

Table 1. Summary of architectural elements and lithofacies observed in the Galho do Miguel Formation

Architectural element	Lithofacies	Description	Interpretation
Compound sets of cross-strata	Sets of cross-strata	Cosets of sandstone cross-strata, 0.8-6 m thick, bounded by erosional surfaces and containing tangential-bottom foresets. They form tabular bodies 4.5 to 13.5 m thick, and more than 500 m in extent in the palaeowind direction. Four orders of erosional bounding surfaces were recognised in this element type.	Transverse draas with out-of-phase sinuous crestline and superimposed smaller transverse dunes with uniform trend towards ENE.
Simple sets of cross-strata	Large-scale simple set of cross-strata.	Single sets, 0.5 to 5 m thick, of concave-up tangential to the bottom cross-strata. They form beds with slightly concave-up bottom and planar top, more than 500 m long in the palaeowind and c. 350 m long perpendicular to that. Compound cross-strata and planar-parallel laminated strata are interlayered with this element.	Simple, isolated and larger transverse dunes with slightly sinuous crestline, migrating towards E direction on a dry depositional surface.
	Small-scale simple set of cross-strata.	Single sets, 0.1 to 2 m thick, of concave-up cross-strata that are tangential to the bottom, and that are more than 150 m long in the palaeowind and 8-40 m long perpendicular to that. Beds exhibit pronounced concave-up bottoms, and are commonly interlayered with wavy and planar-parallel bedded sandstone and irregular horizontally beds.	Simple, isolated and smaller transverse dunes. Geometry and spread direction of the foreset azimuths suggest pronounced sinuous crestline and migration toward the NE sector. These small dunes formed on a damp/wet surface.
Planar-parallel sandstone strata	Planar, parallel-laminated, fine- and medium-grained sandstone.	Planar, or low-angle (up to 4°), parallel strata, 1 to 20 mm thick. In thin section, it is possible to observe laminae with a crude inverse grading. These sedimentary structures form 0.5-6.5 thick beds and more than 500 m in lateral extent.	These laminae correspond to subcritically climbing translatent strata (Hunter, 1977) deposited by climbing wind ripples on a dry interdune or interdraa flat surfaces.
Wavy and planar-parallel bed sandstone	Planar, parallel-laminated, sandstone.	Horizontal, or low-angle (up to 4°), parallel strata, 1 to 20 mm thick.	This corresponds to subcritically climbing translatent strata (Hunter, 1977) formed by climbing wind ripples on a flat surfaces temporarily dry. .
	Wavy laminated sandstone	On the bedding surface, this lithofacies consists in symmetrical ripples with rectilinear and bifurcate crests. In section, climbing symmetrical cross-laminations are observed.	Vortex ripples produced by wind-induced small wave in shallow ponds.
	Adhesion ripples	On the bedding surface, this lithofacies consists in small asymmetrical microridges. In section, it exhibits of tabular sets of weakly undulated and irregular cross-strata that are up to 60 mm thick.	Small and isolated adhesion ripples formed on a damp surface.
Irregular horizontal beds	White irregularly horizontal layers	Very fine- to fine-grained sandstone forming (i) small irregular patches, (ii) small concave-up lenses that are evenly spaced, (iii) thin discontinuous horizontal layers, (iv) isolated concave-up lenses, (v) humpbacked lenses and (vi) wavy lenses.	The lithofacies (i) to (iv) are the depositional product of the interaction of efflorescence crust of evaporite deposits (now dissolved) and aeolian or subaqueous depositional processes. See the text for a detailed interpretation. The lithofacies (v) consists in vortex ripples produced by wind-induced small wave in shallow ponds
	Light grey irregularly horizontal layer	Structureless muddy sandstone forming beds that are 5-150 mm thick and with lateral extent of more than 30 m.	Fine-grained wind-blown material that adhered on damp hygroscopic surfaces of the salt crusts and was deposited after their dissolution.

Declaration of interests

x The authors declare that they have no known competing financial interests or personal relationships that could have appeared to influence the work reported in this paper.

☐The authors declare the following financial interests/personal relationships which may be considered as potential competing interests:

AUTHOR STATEMENT

Dear Editor,

Nothing different than is written in Cover Letter.

Giorgio Basilici, Aquila Ferreira Mesquita, Marcus Vinicius Theodoro Soares, Juraj Janocko, Nigel Philip Mountney and Luca Colombera